

To Model Chemical Reactivity in Heterogeneous Emulsions, Think Homogeneous Microemulsions

Carlos Bravo-Díaz,^{*,†} Laurence Stuart Romsted,^{*,‡} Changyao Liu,[‡] Sonia Losada-Barreiro,[†] María José Pastoriza-Gallego,[§] Xiang Gao,[‡] Qing Gu,[‡] Gunaseelan Krishnan,[‡] Verónica Sánchez-Paz,[†] Yongliang Zhang,[‡] and Aijaz Ahmad Dar^{||}

[†]Universidade de Vigo, Facultad de Química, Departamento Química Física, 36200, Vigo, Spain

[‡]Department of Chemistry and Chemical Biology, Rutgers, The State University of New Jersey, New Brunswick, New Jersey 08854, United States

[§]Departamento Física Aplicada, Facultad Química, Universidad de Vigo, 36200 Vigo, Spain

^{||}Department of Chemistry, University of Kashmir, Hazratbal, Srinagar, J&K India

Supporting Information

ABSTRACT: Two important and unsolved problems in the food industry and also fundamental questions in colloid chemistry are how to measure molecular distributions, especially antioxidants (AOs), and how to model chemical reactivity, including AO efficiency in opaque emulsions. The key to understanding reactivity in organized surfactant media is that reaction mechanisms are consistent with a discrete structures—separate continuous regions duality. Aggregate structures in emulsions are determined by highly cooperative but weak organizing forces that allow reactants to diffuse at rates approaching their diffusion-controlled limit. Reactant distributions for slow thermal bimolecular reactions are in dynamic equilibrium, and their distributions are proportional to their relative solubilities in the oil, interfacial, and aqueous regions. Our chemical kinetic method is grounded in thermodynamics and combines a pseudophase model with methods for monitoring the reactions of AOs with a hydrophobic arenediazonium ion probe in opaque emulsions. We introduce (a) the logic and basic assumptions of the pseudophase model used to define the distributions of AOs among the oil, interfacial, and aqueous regions in microemulsions and emulsions and (b) the dye derivatization and linear sweep voltammetry methods for monitoring the rates of reaction in opaque emulsions. Our results show that this approach provides a unique, versatile, and robust method for obtaining quantitative estimates of AO partition coefficients or partition constants and distributions and interfacial rate constants in emulsions. The examples provided illustrate the effects of various emulsion properties on AO distributions such as oil hydrophobicity, emulsifier structure and HLB, temperature, droplet size, surfactant charge, and acidity on reactant distributions. Finally, we show that the chemical kinetic method provides a natural explanation for the cut-off effect, a maximum followed by a sharp reduction in AO efficiency with increasing alkyl chain length of a particular AO. We conclude with perspectives and prospects.

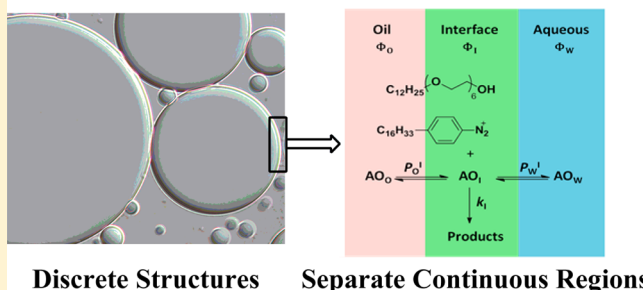
I. INTRODUCTION

"How wonderful that we have met with a paradox. Now we have some hope of making progress."¹

About 20 years ago, William Porter aptly stated the polar paradox that characterized an apparent contradiction in the current state of knowledge about polar and nonpolar antioxidant (AO) efficiencies in different reaction media:

"[N]onpolar antioxidants or amphiphilic antioxidants of low HLB [hydrophilic-lipophilic balance] function relatively best in polar lipid emulsions and membranes of high surface to volume ratio while polar antioxidants (or amphiphiles of high HLB) are relatively more effective in bulk lipids of low surface/volume ratio."²

Aggregate Structure-Reaction Region Duality



Discrete Structures Separate Continuous Regions

Understanding AO efficiency in emulsified foods or in biological systems requires the development of mechanistic models for the effect of AOs on inhibiting peroxidation in organized media. This is a challenging problem because the site of reaction is often uncertain, more than one mechanism may occur, the distribution of reactive components is uncertain, and the concentrations of reactants in the different reaction regions have not been determined.³

Received: January 11, 2015

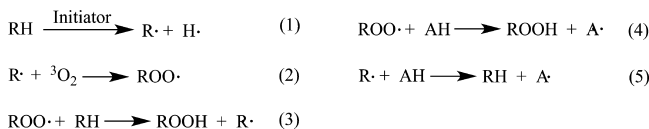
Revised: March 21, 2015

Published: March 25, 2015

Over the past several decades, a number of research groups have contributed to solving these problems. For example, one proposed peroxidation mechanism is a multistep chain reaction.⁴

Scheme 1 illustrates several parts of this mechanism, including initiation step (1) by the formation of a radical at a carbon alpha

Scheme 1. Initial Steps in the Chain Mechanism of Peroxidation of Unsaturated Lipids (Equations 1–3) and Termination of Peroxidation by an Antioxidant, AO (Equations 4 and 5)



to a double bond on a hydrocarbon and chain propagation steps (2 and 3), including the addition of $^3\text{O}_2$ followed by transfer of a hydrogen to the terminal oxygen by another unsaturated hydrocarbon. (Other chain propagation and termination steps are not shown.) Steps (4) and (5) show the transfer of a hydrogen to a peroxy radical or carbon radical from a phenolic compound to give a phenol radical that is more stable than the peroxy radical. Scheme 1 illustrates only a small fraction of the complexity of understanding the effect of antioxidant (AO) mechanisms of peroxidation in unsaturated oils. For example, see Figure 2 in ref 5. Additional details are in reviews and book chapters.^{3,4,6,7}

Because of the inherent difficulties in determining AO distributions in opaque emulsions using the peroxidation reaction itself, we decided to determine AO distributions via a chemical kinetic method that is based on the reaction of AOs with hydrophobic 4-hexadecylarendiazonium ions, 16-ArN_2^+ (prepared as its BF_4^- salt), and grounded in the well-established pseudophase kinetic model (see below). The reaction of an AO, e.g., *t*-butylhydroquinone, TBHQ, with 16-ArN_2^+ is illustrated in Scheme 2. This approach avoids having to determine the distributions of AOs, peroxides, and unsaturated oils by physical methods or to determine the mechanism of their reactions with an AO in microemulsions or emulsions such as the potential homolytic cleavage products (Scheme 3 below).⁸

The application of chemical kinetics and pseudophase models to determining AO distributions in intact opaque emulsions evolved out of our prior contributions to interpreting the chemical reactivity and the realization that reactant diffusion in emulsions could approach the diffusion-controlled limit and be in dynamic equilibrium just as in homogeneous association colloids including micelles, microemulsions, and vesicles.⁹ Traditionally, organized media such as homogeneous aqueous solutions of association colloids are modeled as pseudophases in which the totality of the aggregates is treated conceptually and mathemati-

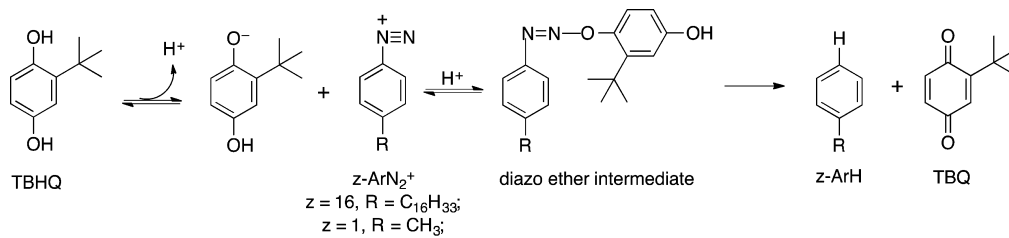
cally as a separate phase, or pseudophase, dispersed in the surrounding aqueous pseudophase.¹⁰ We realized that kinetic models originally developed for association colloids might also work for emulsions because the emulsions are often sufficiently kinetically stable that they do not phase separate during a reaction or because their component distributions are maintained at equilibrium by simple stirring.⁹

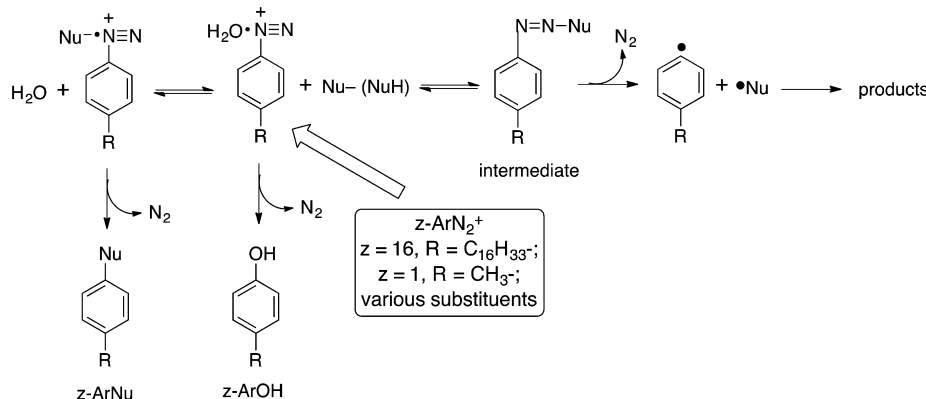
Changes in aggregate size and shape and their effects on chemical reactivity are not included directly in any pseudophase model. Indeed, evidence for droplet size effects on the rates of reaction in emulsions never materialized in our results. The rate of thermal reactions is orders of magnitude slower than molecular diffusion, the reactant distributions are in dynamic equilibrium throughout the emulsion, and their observed rates of reaction show a similar dependence on the total volume of surfactant in solution just as in association colloids.^{10,11} Aggregate size and shape do not need to be known, just as in microemulsions.⁹ See the duality discussion below and in Supporting Information, S1.

Emulsions are opaque, and many common instrumental methods used to monitor reactions in transparent solutions do not work in emulsions. We developed a chemical probe, an arendiazonium ion, 16-ArN_2^+ , that reacts with AOs only in the interfacial regions of emulsions and also two methods for following the loss of 16-ArN_2^+ over time in emulsions, linear sweep voltammetry, and dye derivatization. We demonstrated that kinetic models for reactivity in microemulsions work equally well in emulsions if they are sufficiently kinetically stable, a requirement that is met by simple stirring.

The following sections introduce (a) the application of pseudophase models to microemulsions and emulsions and their division into three reaction regions with distinct properties: oil, interfacial, and aqueous; (b) why emulsion and microemulsion properties are essentially the same on the molecular level in terms of treating chemical reactions occurring within them; (c) the logic of the chemical kinetic approach is developed in some detail, including the basic assumptions, the equations used to represent them, and the evidence that supports them; and (d) why pseudophase models work in systems formally composed of two phases (See Supporting Information S2 for the details of our assumptions.) Later sections provide examples of published results that illustrate what has been learned by the approach and the range of its applications, including two recent examples of how the method provides a natural explanation of the “cut-off” effect.¹² Future directions focus on (a) the factors that control AO distributions in association colloids and emulsions, e.g., AO polarity, charge, and structure and how the distributions correlate with their efficiencies, and (b) how AO distributions affect their tendency to act as prooxidants or synergists. These issues and other research directions are discussed in section VII.

Scheme 2. Reaction of 16-ArN_2^+ with TBHQ in the Interfacial Region of an Emulsion Showing the Deprotonation of TBHQ and the Formation of the Diazoether Intermediate and Products *t*-Butylquinone, TBQ, and Hexadecylbenzene, 16-ArH



Scheme 3. Effect of Nucleophile Basicity on the Reaction Mechanism of Arenediazonium Ions^a

^a(Right-hand side) More basic nucleophiles react at the terminal nitrogen to form $\text{R}-\text{Ar}-\text{N}=\text{N}-\text{Nu}$ adducts. Good nucleophiles but relatively poor leaving groups form intermediates of variable stability such as with anions of antioxidants (e.g., *t*-butylhydroquinone and ascorbic or gallic acids). Some stabilization occurs by conversion to a thermodynamically stable isomer ($Z-E$ isomerization). In some circumstances, isomerization is not possible and the adduct splits homolytically to give reduction products. (Left-hand side) Nucleophiles that are weak bases or good leaving groups such as halide or acetate ions do not react directly with the terminal nitrogen but undergo spontaneous decompositions from cation–nucleophile pairs.

Ia. Similarities and Differences: Micelles and Vesicles.

Micellar solutions usually contain two components and sometimes other additives such as salts and alcohols. Vesicular solutions are similar except that the surfactant generally has two tails and forms spherical bilayers that contain a water pool. That is, both the inside and outside interfacial regions are like micellar surfaces. The hydrocarbon tails make up the cores of vesicles and micelles, and the interfacial and core regions occupy, very approximately, about 50% each of the total aggregate volume. In partitioning and kinetic experiments, both vesicles and micelles are treated as pseudophases in which the totality of the aggregates is treated as a single phase accessible to the reactants and in which reactants are either bound or free, a two-site (or region) model. Reactants are typically polar organic molecules (reactive functional groups generally have some polarity) and are assumed to be associated with the micelle or vesicle aggregates as a whole and not specifically in the interfacial region or micellar core.

Ib. Microemulsions. Figure 1 is a pseudoternary phase diagram for a hypothetical three-component oil, water, and surfactant system.¹¹

The open areas in the diagram are homogeneous microemulsions or mesophases, and the various aggregate structures shown are present at different weight percents of the three components. (Note that any point within the diagram indicates the composition of the three components at that point.) The structures and their sizes and shapes are determined by a variety of physical methods.¹³ Lined areas are biphasic, and dark-gray areas are triphasic. The three borders, at which one component concentration is zero, are two-component systems. The solid black line extending from a 50:50 surfactant/water ratio at 0% oil on the left to 100% oil in the lower right corner provides some examples of changes in the phase states and aggregate structures with added oil. Note that the oil region in aqueous microemulsions may be much larger than the volume occupied by the tails of surfactants in micelles or vesicles. The surfactants typically have hydrocarbon tails covalently linked to headgroups that may be nonionic or ionic. Most of the surfactants used in the results summarized here are nonionic (Chart 1), but a few are cationic (anionic counterions), anionic (cationic counterions), or zwitterionic. “Water” means aqueous solutions that may contain

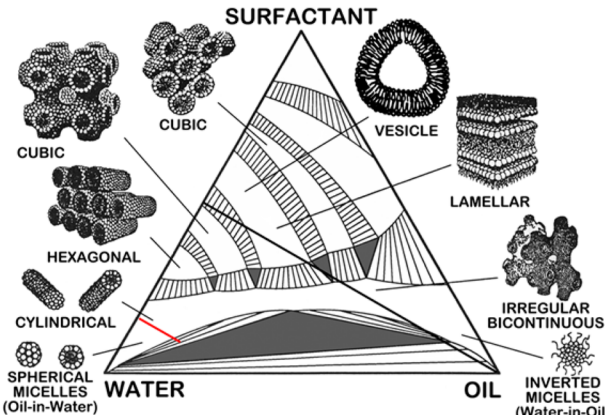
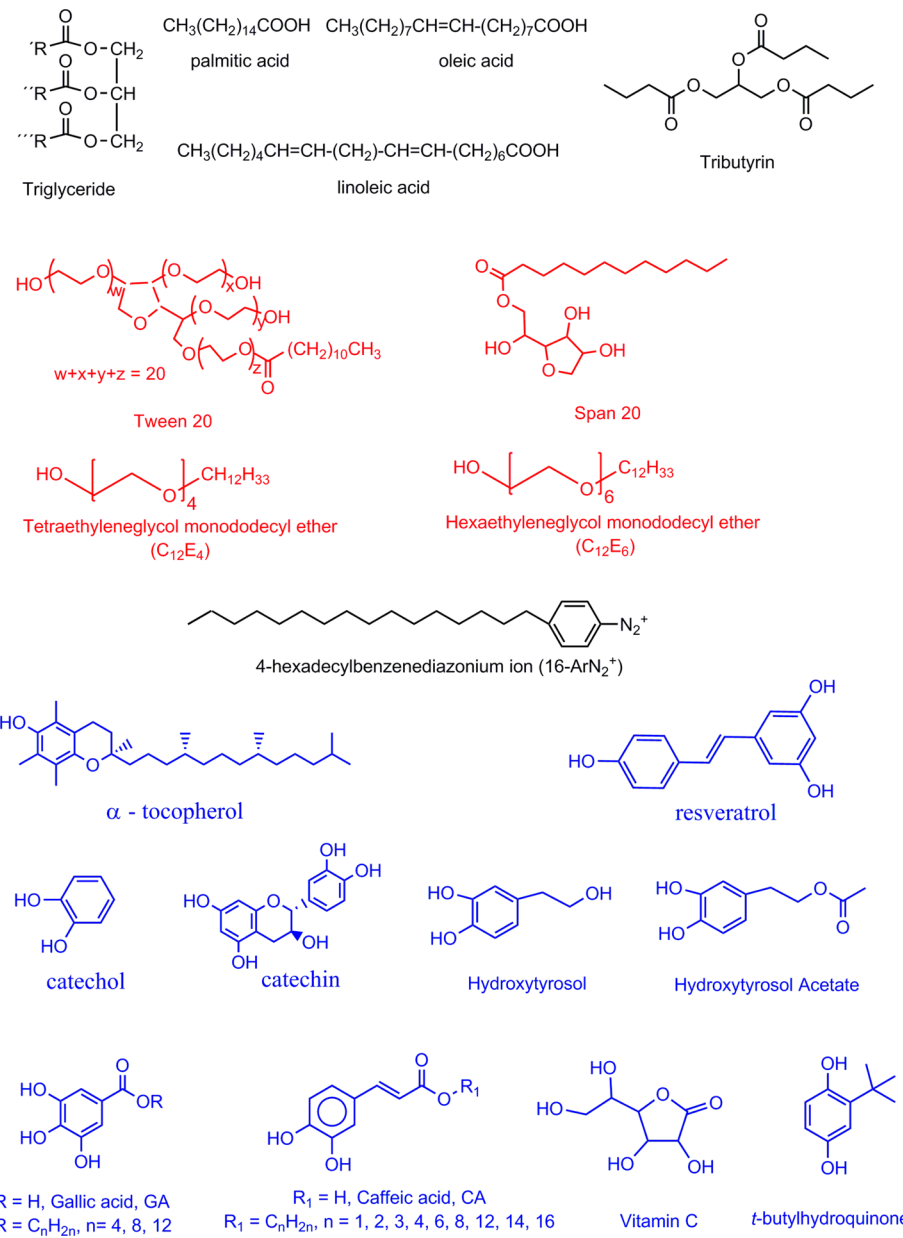


Figure 1. Hypothetical ternary phase diagram for a three-component system of water, oil, and surfactant illustrating the images of various aggregate structures. The open regions are homogeneous mesophases. Aggregate structures are determined by scattering methods. The images distort reality because the structures are much larger than the surfactant molecules and on the molecular level the surface curvatures, except for those in the micelle corners, are quite small. Redrawn from ref 11 with permission from the American Institute of Physics.

other components, e.g., buffers or salts or surfactant monomer. Stirring the mixtures in the bi- and triphasic regions creates metastable emulsions of short (some salad dressings) to long lifetimes (mayonnaise).

The mesostructures in any homogeneous regions of Figure 1 contain large numbers of molecules in the oil, surfactant, and water regions. Although these regions are much larger than single molecules, they are smaller than the total mixture. Each homogeneous region differs in the amounts of oil, surfactant, and water present, in aggregate shapes and in the net balance of forces controlling their stabilities. The underlying structural commonality of all of these mesophases is a surfactant region that separates oil and water regions such that the local polarity drops from that of water to hydrocarbon across the headgroup region, ca. 1 nm. Our research is currently focused on the microemulsion/emulsion area in the lower left of Figure 1 that contains

Chart 1. Structures of Oils, Surfactants, the Probe, and Antioxidants Discussed in This Article



oil-in-water droplets of various shapes, from the water corner toward the middle of the diagram, e.g., a 1:1 oil/water volume ratio with a surfactant concentration $\leq 5\%$ by weight.

Ic. Emulsions. The aggregates in the homogeneous region in the water corner are composed of, metaphorically, oil-bloated microemulsion droplets in which the amount of surfactant is sufficient to fully solubilize the oil. Imagine adding oil to a fluid homogeneous microemulsion composition in Figure 1 that is directly adjacent to a two-phase region. As the oil content is increased and surfactant and water are removed at a constant surfactant/water ratio, the composition will cross a phase boundary and the homogeneous microemulsion will become a true two-phase system, e.g., Figure 1, short red line. Stirring such mixtures may produce emulsions of various stabilities. At the molecular level, however, the primary difference between the initial oil-in-water microemulsion and the emulsion is caused by relatively small changes in the stoichiometric concentrations of

the three components. Small amounts of additives, e.g., reactants, will have little effect on the transition boundary.

Id. Molecular Interactions in Microemulsions and Emulsions: Dynamic Equilibrium. After bulk mixing of homogeneous microemulsions or heterogeneous emulsions, distributions of reactants in thermal reactions are determined by their relative solubilities in each region—oil, interfacial, and aqueous—and their reactions are not limited by diffusion. In organized media, molecules and ions exchange rapidly because the various noncovalent Coulombic, hydration, acid/base, hydrogen bonding, dipole, dispersion, and polarization interactions are weak compared to covalent bonds or complexes with a fixed stoichiometry. Nevertheless, the high cooperativity driven by an increase in entropy of the system and multiple weak intermolecular interactions are sufficient to maintain the oil, interfacial, and water organization.^{10,11} When the bulk composition is changed in a three-component system, both the number of intermolecular and ionic interactions and the number

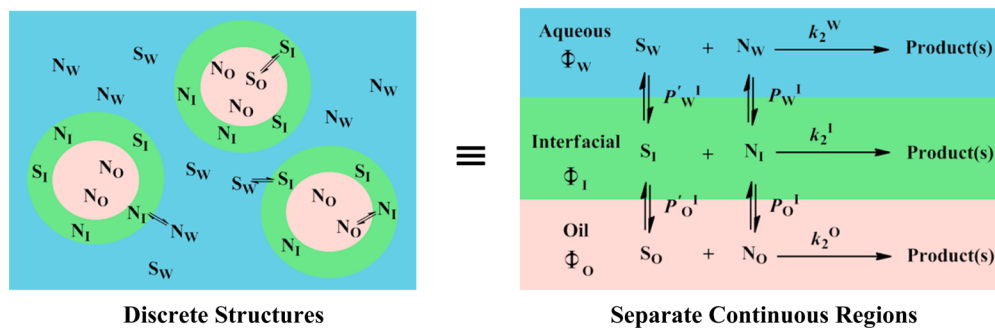


Figure 2. Illustration of equivalent reactant distributions based on the pseudophase model. S and N are in dynamic equilibrium among the oil, interfacial, and aqueous regions of a microemulsion or emulsion. (Left) Emphasizes the exchange between droplets. (Right) Emphasizes the exchange among the totalities of the three regions and also contains a kinetic scheme that is consistent with the Acree–Curtin–Hammett principle (see the text) for a bimolecular reaction between S and N that occurs concurrently in all three regions of a microemulsion or emulsion. Also represented are three volume fractions (Φ_W , Φ_I , and Φ_O), the second-order rate constants in each region (k_2^W , k_2^I , and k_2^O), and the two partition constants (P'_W^I and P'_O^I).

and shapes of the mesostructures may change. However, because the oil, surfactant, and aqueous components are identical throughout the phase diagram, there is no reason to expect that small differences in emulsion composition on either side of a two-phase boundary should produce a dramatic difference in the rates of diffusion of the molecules, e.g., from near the diffusion-controlled limit in the homogeneous region to orders of magnitude slower in the two-phase region.

II. MODELING CHEMICAL REACTIVITY IN ORGANIZED MEDIA

IIa. Starting Point: Treating Bimolecular Reactions in Aqueous Solution. In general, the treatment of chemical reactions in surfactant solutions begins with the rate law for bimolecular reactions, e.g., substrate, S, and reactant, N, in bulk solution (eq 1)

$$\text{rate} = -\frac{d[S_T]}{dt} = k_2[S_T][N_T] = k_{\text{obs}}[S_T] \quad (1)$$

where $k_{\text{obs}} = k_2[N_T]$, k_2 is the second-order rate constant ($M^{-1}s^{-1}$), $[S_T]$ stands for the total, initial, or stoichiometric concentration, and square brackets in general indicate mol/L of the total solution volume here and throughout the text. When the second reactant is present in large excess, $[N_T] \gg [S_T]$, the observed rate is expressed by a first-order rate constant, k_{obs} (s^{-1}). The definitions of the rate of the reaction in equation 1 are also used to define the rate of reaction in reactive regions of micelles, vesicles and microemulsions and the oil, interfacial and aqueous regions of emulsions.

Equation 1 separates the observed rate of reaction into a second-order rate constant or coefficient whose value depends on the medium effects on the reaction's free energy of activation and concentration terms for S and N. Many reactions are first order with respect to each reactant concentration. Bimolecular reactions in solutions are generally run in excess N_T , which means that $[N_T]$ remains constant throughout the time course of the reaction. This experimental condition simplifies the interpretation of the kinetic data considerably. The change in concentration of S_T with time can be measured by a variety of standard methods. Values for k_{obs} and k_2 are obtained from the linear integrated first-order rate plot or by using standard computer fitting methods on the exponential form of the kinetic data. To simplify the interpretation of micellar effects, reactions chosen for studies were generally those with established mechanisms. Values of k_2 determined in different solvents

provide important information on solvation effects on organic reactions. In micelles, values of k_2 for completely bound reactants provide information on the free energy of activation in the interfacial medium that can be compared with k_2 values in other micellar interfacial regions and bulk solvents.^{14,15}

IIb. Pseudophase Kinetic Models: Homogeneous Solutions of Association Colloids. Kinetic models for bimolecular reactions in micellar solutions were introduced more than 40 years ago, initially by Menger,¹⁶ expressed for the first time as a pseudophase model by Yatsimirski and co-workers to account for the distributions of two uncharged reactants,¹⁷ and expanded by Romsted to include ion exchange effects on bimolecular reactions between organic substrates and reactive counterions,^{18,19} and the ion exchange concept was grounded in thermodynamics by Chaimovich and Quina.^{10,20} Progress and applications to microemulsions and vesicles have been reported periodically in numerous review articles.^{14,15,21,22} Over time, pseudophase models in which the micellar or vesicular solution is divided into two reaction regions, aqueous and aggregate, replaced attempts to interpret reactivity in terms of aggregate size and surface potentials by treating homogeneous association colloids as pseudophases and ionic aggregates as selective ion exchangers.

In pseudophase models for microemulsions, the homogeneous solution is divided into three separate continuous reaction regions—oil, interfacial, and water—represented by subscripts O, I, and W, respectively.^{23,24} Figure 2 contains two images of the discrete structures—separate continuous regions duality. (For a fuller description of this concept, see Supporting Information S1.) Figure 2 (left) is a cartoon of oil-in-water microemulsion droplets observed by microscopy and scattering methods such as those often found in relatively dilute solutions in the lower left corner of Figure 1. The image in Figure 2 (left) is iconic. It represents various microemulsion mesophases and emulsion droplets of many sizes (not shown) having boundaries that molecules diffuse across (e.g., AOs) that occur in systems having two- and three-phase regions (Figure 1). In principle, the chemical kinetic method described here for oil-in-water emulsions and microemulsions should work in all three component mesophases if the solutions are sufficiently fluid to ensure uniform bulk mixing, but the method has not yet been tested in them. The volume of the interfacial region, V_I , is the totality of all of the interfacial regions in all of the aggregates within the bulk microemulsion and is set equal to the total volume of added surfactant. The total volume of the oil within

the droplets equals the volume of added oil, V_O , and the total water volume, V_W , determines the volume of the continuous aqueous pseudophase. The volumes of three regions are assumed to be additive and equal to the total volume of the solution, V_T (eq 2):

$$V_T = V_I + V_O + V_W \quad (2)$$

Note that the pseudophase model can, in principle, also be applied to all homogeneous mesophases and the emulsion regions in their vicinity as long as the mixtures are fluid enough to ensure good bulk mixing (Figure 1). Figure 2b provides an image of any homogeneous solution or stirred heterogeneous mixture within the ternary phase diagram (Figure 1), although much of our current work has been done on structures in the lower left corner.

At dynamic equilibrium, the rapidly moving molecules are distributed among three separate continuous regions with distinct physical properties: oil, interface, and aqueous (described below). Both S and N partition among the three regions. The solvation properties of each region are unique, and the solubilities of S and N may be very different in the oil, aqueous, and interfacial regions. This also means that solvent effects on the ground-state and transition-state stabilities of S and N in a reaction may be different in each region. The distributions of S and N are described by thermodynamic partition coefficients, but we use the informal approach of calling them partition constants, just as rate coefficients are called rate constants, between aqueous and interfacial regions for S and N, P'_W^I and P_W^I , and between oil and interfacial regions, P'_O^I and P_O^I , respectively (Scheme 2). (See section IIc for the definitions of the partition constants.) These partition constant definitions are based on an extrathermodynamic assumption because the partitioning occurs within a homogeneous micellar and microemulsion solutions or within a kinetically stable biphasic emulsion and because the interfacial region is not a true phase. The assumption works because the reactant distributions are in dynamic equilibrium (see below). The arenediazonium ion, 16-ArN₂⁺, (Chart 1) used in our experiments is a surfactant-like hydrophobic cation, and its concentrations in the oil and water regions are negligible as noted above. The effect of the structure of N, e.g., systematically changing its hydrophobicity, on its distributions among the three regions is analyzed by comparing the change in the partition constant, P_W^I and P_O^I values.

IIc. Why Does Dynamic Equilibrium Matter in Organized Media? Our approach is related to the Acree–Curtin–Hammett principle in which reactant ground states are rapidly equilibrating.²⁵ Figure 2 (right) shows that the contributions to the measured or observed reaction rate for the three separate reaction pathways in the continuous oil, interfacial, and aqueous regions are proportional to the concentrations of N and S in each region because the rate of reaction of N with S in the interfacial region is orders of magnitude slower than diffusion between regions. Dynamic equilibrium ensures that in kinetically stable or stirred emulsions N and S are distributed throughout the oil, interfacial, and aqueous regions in microemulsions and the distributions reflect their relative solubilities throughout the time course of the reaction. (See section IIc on the mathematical treatment.) Because the volumes of all three regions are large compared to the volumes of added reactants N (e.g., AO) and S (e.g., substrate), the distributions and reactivities are proportional to the volumes of each region and are independent of the size or shape of the oil, interfacial, and aqueous regions. Put differently, the volume of each region determines, in part, the

relative concentration of reactants in each region, i.e., their molarities, and the reaction rates are proportional to molarities. The interfacial regions of nonionic microemulsions and emulsions, for example, contain some oil, water, and polyoxyethylene chains, and differences in shape of large aggregates should not significantly alter the medium properties of the interfacial regions. However, interfacial regions cannot be isolated, and the rate constant within them cannot be determined independently but only by fitting kinetic models to the measured rate constants.

IId. Molecular Diffusion is Really Fast and AOs React with the Arenediazonium Ion Really Slowly. The diffusivities of a number of ions and molecules in homogeneous or surfactant solutions are not too much less (~1 to 2 orders of magnitude) than the hydronium ion, ca. $10 \times 10^{-9} \text{ m}^2 \text{ s}^{-1}$. For example, lysozyme diffuses only about 100 times slower at $7 \times 10^{-11} \text{ m}^2 \text{ s}^{-1}$.²⁶ The rate constant for the diffusion-limited reaction of H₃O⁺ with H₂O is $1 \times 10^{10} \text{ M}^{-1} \text{ s}^{-1}$, and the free energy of activation for proton transfer is less than the free energy of transfer for diffusion together with H₃O⁺ and H₂O.²⁷ This rate constant is equivalent to the diffusivity of the hydronium ion, and the units are interconvertible.²⁸ The second-order rate constants for the entrance of alkyl sulfate surfactant ions into micelles range from $3.2 \times 10^9 \text{ M}^{-1} \text{ s}^{-1}$ (hexyl) to $4.7 \times 10^8 \text{ M}^{-1} \text{ s}^{-1}$ (tetradecyl), differing by less than a factor of 10, whereas the first-order exit rate constants vary about 1000-fold, from $1.32 \times 10^9 \text{ s}^{-1}$ (hexyl) to $9.6 \times 10^5 \text{ s}^{-1}$ (tetradecyl).¹³ The second-order rate constants for the thermal reactions generally studied in our work are many orders of magnitude slower (see below). The half-lives for the diffusions of the molecules are on the nano time scale, but many of the thermal reactions studied in surfactant systems have half-lives on the minutes to hours time scale, 10^2 – 10^4 s, or are 10^6 to 10^9 times slower than diffusion for most molecules and ions.

In principle, the slow step of a reaction may be the diffusion of reactants, but typically this occurs only in viscous media when the reaction between S and N is extremely fast. One study shows that the competitive trapping of Cl⁻ and Br⁻ by three different benzenediazonium ions is not significantly affected by changes in solvent viscosity produced by ethylene glycol or glycerol.²⁹ Unlike thermal reactions, fluorescence and the decay of triplet states and photochemical reactions are on the nanosecond to picosecond time scales, shorter than aggregate lifetimes but similar to or faster than reactant exchange rates between regions.²⁵ The assumption of dynamic equilibrium does not apply to those systems, and the distributions and rates of reactions are sensitive to specific interactions within the aggregates.³⁰

IIe. Pseudophase Models: Reactions in Emulsions. The intermolecular interactions between molecules and ions in emulsions are generally weak, and their diffusivities should be essentially the same as those in the microemulsion regions of the phase diagram for the same components (Figure 1) and orders of magnitude faster than the rates of thermal reactions. Our research on AOs in emulsions over the past decade demonstrates that pseudophase models developed for microemulsions also work in emulsions, provided that the emulsion is either kinetically stable or gently stirred after initial mixing. In summary, as long as dynamic equilibrium holds, the properties of organized systems such as emulsions are like those of association colloids, in particular, microemulsions (see section IIb).

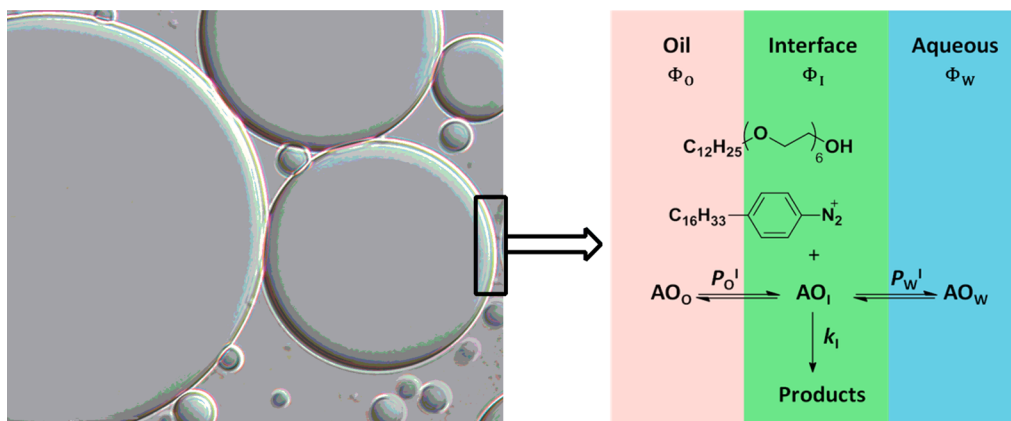


Figure 3. Aggregate structure–reaction region duality. (Left) Image of oil in water droplets on the micrometer scale. These iconic images represent boundaries but not necessarily barriers between regions, some of which are observed by physical methods. (Right) Cartoon of the totality of the oil, O, interfacial, I, and aqueous, W, regions of a microemulsion or emulsion showing the equilibrium partitioning of an AO among the three regions, the oil–interface and water–interface partition constants, the nonionic surfactant, the arenediazonium ion probe (see below), the second-order rate constant in the interfacial region, and the reaction products.

III. INTRODUCTION TO THE CHEMICAL KINETIC METHOD IN EMULSIONS

Figure 3 is a different representation of the discrete structures—separate continuous regions duality for the AO/16-ArN₂⁺ systems that we have studied in emulsions. The left side of Figure 3 is an image of oil-in-water droplets in an emulsion on the micrometer scale,⁹ but the image could equally well be of much smaller droplets in a homogeneous microemulsion. Note that the curvature of these droplets is very high, but relative to the very small size of a single surfactant or reactant molecule, the surfaces are virtually flat (not unlike the imperceptible curvature of the earth when viewed at the earth–air interface as opposed to outer space). The reaction scheme on the right side of Figure 3 summarizes the important chemistry of the chemical kinetic method. An emulsion is composed of, for example, a food oil, a nonionic surfactant, hexadecyl monododecyl ether (C₁₂E₆), an AO, *t*-butylhydroquinone (TBHQ), and the arenediazonium ion (16-ArN₂⁺, the chemical substrate or probe that reacts with the AO). (See Scheme 2.) 16-ArN₂⁺ is used in all determinations of AO partition constants (see below). The reaction scheme in Figure 3 is equivalent to Figure 2 (right), with 16-ArN₂⁺ = S and AO = N. As noted above, 16-ArN₂⁺ has negligible solubility in the aqueous and oil regions because it is both hydrophobic and charged and it reacts with AO only in the interfacial region (section IIIc).

The bulk efficiencies of AOs in inhibiting lipid oxidation depend on the rate constant for the particular chemical reaction and the concentrations of the reactants within the interfacial region, proposed to be the location of reactions in emulsions by Frankel.³¹ The rate of reaction between an AO and peroxy radicals depends upon AO properties such as the O–H bond dissociation energy, steric hindrance, and stability of the resulting radical.^{5,32} For example, catechol derivatives are powerful AOs because of their low oxidation potential, stabilization of the semiquinone radical derived from the H atom by intermolecular hydrogen bonds, and the electron-donating properties of the ortho group.³¹ The mechanisms of lipid peroxidations are now fairly well known in aqueous solution;³³ however, the structural complexities of emulsions have hindered the in-depth analysis of the parameters affecting the AO reactivity and distribution.^{3,6,7}

The pseudophase kinetic model predicts that at constant volume fraction ratios of the oil and aqueous regions, Φ_o/Φ_w ,

[AO_T] and k_{obs} values depend on both [AO_T] as determined by the AO partition constants between the aqueous and interfacial and the oil and interfacial regions (P_w^I , P_o^I), respectively, and on the medium effect of the interfacial region on the rate constant for reaction, k_I (Figure 3). We have developed methods to determine the distributions of the AOs as the percentage of the AO in each region. Our results, obtained with structurally different AOs under a variety of experimental conditions, confirm that P_w^I and P_o^I values depend on a number of emulsion and AO properties and experimental conditions.^{9,34–38} Little is known about the structure–reactivity relationships for k_I .

IIIa. Properties of the 4-Hexadecylbenzenediazonium Ion, 16-ArN₂⁺, as a Chemical Probe. 16-ArN₂⁺ is a unique chemical probe that reacts with AOs via an oxidation/reduction mechanism.⁵ We selected this cation for several reasons: (a) because of the significant level of current understanding of the rich and complex chemistry of arenediazonium ions;³⁹ (b) because we successfully used a structurally similar 2,4-dimethyl-4-hexadecylarenediazonium ion under conditions in which it reacts heterolytically, to monitor the interfacial molarities of a wide variety of weakly basic nucleophiles, including water, in association colloids^{40,41} and to cleave peptide bonds;⁴² (c) because the preparation of 16-ArN₂⁺ and other substituted arenediazonium ions as their fluoroborate (BF₄[−]) salts from their aniline precursors is straightforward^{40,43} and occurs in high yields (>70%); (d) because the reactive group of the cation is located within the interfacial region of the aggregates; and (e) because the oxidation/reduction reaction of 16-ArN₂⁺ with AOs is significantly faster than its spontaneous heterolytic dediazonation in different solvents, association colloids, and emulsions.^{8,44–48}

Scheme 3 summarizes the heterolytic dediazonation and oxidation/reduction pathways.⁸ In aqueous acid solution, in the dark and in the absence of reducing agents, arenediazonium ions decompose spontaneously via the rate-limiting loss of N₂ and react competitively with weakly basic nucleophiles.^{8,40} Our focus here is on the reaction of 16-ArN₂⁺ with AOs as illustrated in Scheme 2 for the reaction of AOs such as *t*-butylhydroquinone (TBHQ), which is first order in 16-ArN₂⁺ and AOs and second order overall.^{8,49} The reaction begins by the diffusion-controlled deprotonation of TBHQ followed by a diffusion-limited reaction with 16-ArN₂⁺ to give a diazoether. In nonionic micelles, the

reaction is run at about pH 3 (e.g., TBHQ, $pK_a = 10.8$), and the reaction is slow enough that it can be monitored on an ordinary UV/vis spectrometer. Observation of the diazo ether intermediate depends on the solution pH and the presence of aggregates.⁸ In association colloids and emulsions at about pH 3, the intermediate is not observed.^{43,50} The reaction of 16-ArN_2^+ with TBHQ gives the reduction product hexadecylbenzene (16-ArH) and the oxidation product *t*-butylquinone (TBQ) (Scheme 2).²⁴ 16-ArH is formed with many different AOs, but the oxidized product of the AO is often unknown or unobserved,⁵ probably because it is in the void volume of the HPLC chromatograms. Its absence does not hinder the determination of the partition constants of AOs with 16-ArN_2^+ . Details are in the references.^{8,40}

IIIb. Mathematical Treatment of Chemical Reactivity in Microemulsions and Emulsions. Equation 3 is a general expression for k_{obs} , based on Figure 2 (right), which is the sum of separate reactions occurring in the oil, interfacial, and aqueous reaction regions for a bimolecular reaction between S and N, with $[N] \gg [S]$, and in which the reactants are in dynamic equilibrium

$$-\frac{dS}{dt} = k_{\text{obs}}[S_T] = k_2[S_T][N_T] = k_O(S_O)(N_O)\Phi_O + k_I(S_I)(N_I)\Phi_I \\ + k_w(S_w)(N_w)\Phi_w \quad (3)$$

where $\Phi_O + \Phi_I + \Phi_W = 1$, $\Phi_O = V_O/V_T$, $\Phi_I = V_I/V_T$, and $\Phi_W = V_W/V_T$ are from eq 2. k_2 is the observed second-order rate constant with $k_{\text{obs}} = k_2[N_T]$; k_O , k_I , and k_w are the second-order rate constants in the oil, interfacial, and water regions; and Φ is the volume fraction of a region. Square brackets indicate moles per liter of total emulsion volume, and parentheses indicate moles per liter of regional volume. The rate of reaction within a region depends on the totality of that region's volume and not on the total solution volume. The volumes of these regions are set equal to the volumes of added aqueous solution, surfactant, and oil (eq 2). The interfacial region is composed of surfactant headgroups and some oil and water interacting with the surfactant. The volume in the interfacial region available to 16-ArN_2^+ and to an AO is uncertain but should be proportional to Φ_I .

IIIc. Determining AO Distributions in Microemulsions and Emulsions by the Chemical Kinetic Method. The general aim of our approach is to determine the distributions of an AO in an emulsion as expressed by its P_W^I and P_O^I values (Figures 2 and 3) from changes in k_{obs} versus surfactant volume fraction Φ_I .

Because the reactive group of 16-ArN_2^+ is located only in the interfacial region (Figure 3), the oil and water concentrations of 16-ArN_2^+ are negligible, i.e., $[16\text{-ArN}_2^+)_O]$ and $[16\text{-ArN}_2^+)_W] \approx 0$, and eq 3 reduces to eq 4 after setting $S_I = (16\text{-ArN}_2^+)_T$ and $N_I = (AO_I)$.

$$-\frac{d[16\text{-ArN}_2^+]}{dt} = k_{\text{obs}}[16\text{-ArN}_2^+)_T = k_2[16\text{-ArN}_2^+)_T[AO_T] \\ = k_I(16\text{-ArN}_2^+)_T(AO_I)\Phi_I \quad (4)$$

Fitting the experimental results also provides an estimate of k_I for the AO. In general, two pieces of information are required, plots of k_{obs} versus Φ_I at constant Φ_O/Φ_W and a value for the partition constant of the AO between oil and water in the absence of surfactant, P_O^W . But simplifications can sometimes be made depending on the hydrophilic/hydrophobic balance of the AO (see below).

IIId. Monitoring the Reaction Between an AO and 16-ArN_2^+ by the Dye Derivatization and Linear Sweep Voltammetry (LSV) Methods. Logarithmic plots of absorb-

ance (dye method) and current (LSV) versus time from both methods were generally linear for 3 to 4 half-lives and first order. See Supporting Information, sections S3 and S4, for a brief description of the methods and example results. Fuller's discussion of the two methods, including limitations, are published.^{50,51}

IIIe. Derivations of the Equations Used in the Chemical Kinetic Method. To apply eq 4 to chemical reactions in emulsions, the right-hand term for reaction in the interfacial region must be converted to measurable stoichiometric concentrations, and several definitions are needed. Details about the derivation are in the Supporting Information, section S5.

Equations 5 and 6 define the partition constants for the distributions of AOs between the aqueous and interfacial, P_W^I , and oil and interfacial, P_O^I , regions.

Combining eqs 4–6 with a mass balance equation for the AO (not shown) gives eq 7:

$$P_W^I = \frac{(AO_I)}{(AO_W)} \quad (5)$$

$$P_O^I = \frac{(AO_I)}{(AO_O)} \quad (6)$$

$$k_{\text{obs}} = k_2[AO_T] = \frac{[AO_T]k_I P_O^I P_W^I}{\Phi_O P_W^I + \Phi_I P_O^I P_W^I + \Phi_W P_O^I} \quad (7)$$

The variation in Φ_I is small (up to 5% by volume); Φ_O and Φ_W are large and approximately constant; in the experiments, the ratio Φ_O/Φ_W is held constant; and k_{obs} decreases with added surfactant, Φ_I .

Equation 7 requires that the value of k_{obs} decreases with added surfactant, i.e., increasing Φ_I because this term appears only in the denominator. However, how rapidly the value of k_{obs} decreases with Φ_I depends on both Φ_O and Φ_W , whose values can be changed experimentally. The detailed treatment and specific equations obtained from eq 7 used to calculate the partition constants are given in the Supporting Information, section S5.1. The two partition constants P_O^I and P_W^I appear as a product term, $P_O^I P_W^I$, in eqs 7 and s11, which is derived from eq 7. Independent values of these two partition constants cannot be obtained from a single set of k_{obs} – Φ_I kinetic data. A second set of kinetic data can be obtained at a different Φ_O/Φ_W ratio, and the two equations can be solved for the partition constants from two equations in two unknowns.

However, we have found that a second approach based on the equalities shown in eq 8 is considerably easier to use as the second equation. P_O^I and P_W^I values are related to the partition constants between the oil and water phases, P_O^W , in the absence of added surfactant, i.e., at $\Phi_I = 0$. Both equations s11 and 8 contain the extrathermodynamic assumption that partition constants within an emulsion or a microemulsion are equivalent to partition constants in true two-phase systems. Once a value P_O^W is obtained, eqs s11 and 8 are solved as two equations in two unknowns.

$$P_O^I = \frac{(AO_W)}{(AO_O)} = \frac{\frac{(AO_I)}{(AO_O)}}{\frac{(AO_I)}{(AO_W)}} = \frac{(P_O^I)}{(P_W^I)} \quad (8)$$

Table 1. Representative Values of Partition Constants, P_W^I and P_O^I , and Interfacial Rate Constants, k_I , Obtained in Emulsions Composed of Acidic Water and Different Oils and Emulsifiers^{a,b}

no.	AO	oil	o/w	T (°C)	pH	emulsifier	HLB emulsifier	P_W^I	P_O^I	$10^2 k_I (\text{M}^{-1} \text{s}^{-1})$
1	CA ²	olive	1:9	25	3.65	TW(20)	16.7	406		3.80
2	CA ³	corn	1:9	25	3.65	TW(20)	16.7	301		2.97
3	CA ³	corn	4:6	25	3.65	TW(20)	16.7	270		3.52
4	CA ³	corn	1:9	25	3.05–3.97	TW(20)	16.7	475–194		0.76–8.16
5	GA ⁴	corn	1:9	25–35	3.7	TW(20)	16.7	121–127		5.4–12.8
6	RES ⁵	corn	2:3	25	2.0	TW(20)	16.7	4374	930	3.02
7	GA ⁶	corn	1:9	25	3.65	TW(20,40,80)/SP(20)	16.7–8.05	123–141		5.3–2.1
8	PG ⁶	corn	1:9	25	3.65	TW(20,40,80)/SP(20)	16.7–10.6	176–522	209–622	19.7–8.5
9	TOC ⁷	corn	1:9	25	3.6	TW(20)	16.7		11.9	17
10	TOC ⁷	olive	3:7	25	3.6	TW(20)	16.7		28.6	19
11	TOC ⁶	corn	1:9	25	3.7	TW(20,40,80)/SP(20))	16.7–8.6		11.3–6.1	17–5
12	TOC ⁸	oct	1:9	15–30	2.5	C ₁₂ E ₆			52–75	0.34–1.71
13	VC ⁹	oct	1:4	25	2.0–3.0	C ₁₂ E ₆		25–4		0.6–2.6

^aLow–high numbers indicate a range in partition and rate constant values obtained over a range of experimental conditions. For example, for no. 4, the range of P_W^I values depends on the range of experimental pH values. See the text for details. ^bCA, caffeic acid; GA, gallic acid; RES, resveratrol; PG, propyl gallate; TOC, α -tocopherol (vitamin E); VC, ascorbic acid (vitamin C); oct, octane; TW(20), Tween 20; and TW(20,40,80)/SP(20), blends of Tweens (20, 40, 80) and Span 20. C₁₂E₆, hexaethylene glycol monododecyl ether.

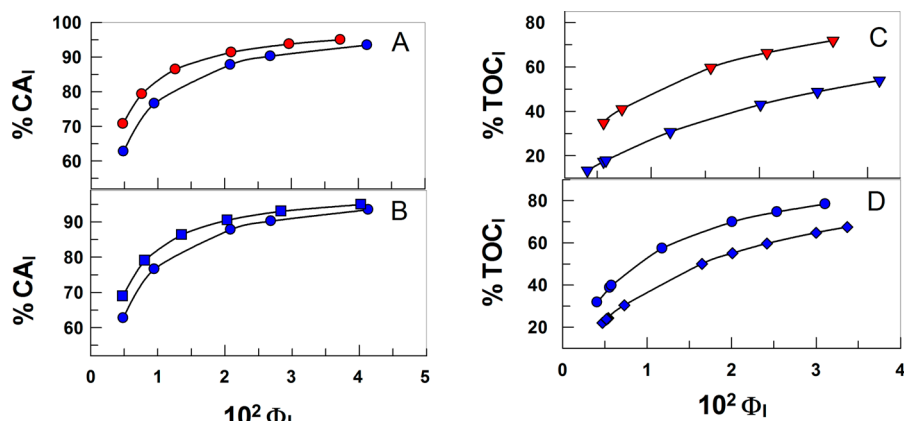


Figure 4. Effects of surfactant concentration, the nature of the oil (corn: blue symbols, olive: red symbols), and the oil/water ratio on the percentages of caffeic acid (CA)⁵³ and α -tocopherol (TOC)³² in the interfacial regions of (A) 1:9 (v/v) emulsions prepared with Tween 20 and corn (blue ●) and olive (red ●) oils; (B) corn oil/Tween 20 emulsions of (●) 1:9 and (■) 2:3 (v/v) oil/water; (C) 3:7 (v/v) emulsions prepared with Tween 20 and corn (▼) and olive (red ▼) oils; and (D) corn oil/Tween 20 emulsions of (●) 1:9 and (♦) 1:4 (v/v) oil/water, pH ~3.7, temperature = 25 °C.

Some typical plots of k_{obs} versus Φ_I are shown for the temperature dependence of k_{obs} on Φ_I for two different antioxidants in the Supporting Information, Figure S3.

IV. EFFECTS OF STRUCTURAL AND ENVIRONMENTAL CONDITIONS ON THE DISTRIBUTIONS OF AOS

Our chemical kinetic method provides a powerful tool for probing AO structure/reactivity relationships in the oil, water, and interfacial regions of emulsions.^{9,34–38} The pseudophase kinetic model predicts that, at constant Φ_O , Φ_W , and $[\text{AO}_T]$, k_{obs} values depend on both distribution (P_W^I , P_O^I) and medium (k_I) effects (eq 7). Values of k_I are not needed to determine partition constants or obtain estimates of AOs distributions, but a comparison of their k_I values under different experimental conditions is important because, as we show below, they afford insights into factors that affect reaction rates in the interfacial region of emulsions. We developed equations for calculating the distribution of AOs as the %AO in each region, but if needed, their concentrations can be estimated by including the volume fraction of each region (Supporting Information, section S5).

IVa. AO Structure/Partition Constant Relationships.

Table 1 lists a number of published values for partition constants in a variety of emulsions. Partition constants of AOs between different regions within emulsions depend on differences in the solvation of the molecules, e.g., the strengths of intra- and intermolecular hydrogen bonding in the various regions. This balance cannot be evaluated solely on the basis of the AO's molecular structure and must be assessed for each AO, oil, and surfactant. In general, P_W^I and P_O^I values are greater than 1 for all AOs investigated from values as low as $P_W^I \approx 4$ (ascorbic acid, vitamin C, VC) or $P_O^I \approx 6$ (α -tocopherol, vitamin E, TOC) up to values of about 1000 and greater, e.g., $P_W^I \approx 4500$ and $P_O^I \approx 950$ (resveratrol, RES). These P_W^I and P_O^I values mean that the free energy of transfer of AOs from the oil and aqueous regions to the interfacial region is negative, i.e., AOs have greater solubilities in the interfacial region than in the oil or water regions and show a strong natural tendency to locate in the interfacial regions, as pointed out by Frankel in 1994,⁵² despite their relatively small fractions of emulsion volumes (ca. $\leq 5\%$ surfactant) compared to oil and water volumes. In summary, AOs with high P_W^I and P_O^I

values tend to have low solubilities in both oil and water and are primarily located in the interfacial region of the emulsions.

IVb. AO Hydrophobicity, Oil Type, Oil/Water Ratio, and HLB Effects on the Distributions of Caffeic Acid and α -Tocopherol AOs. Caffeic acid (CA, Chart 1) is hydrophilic and oil-insoluble and partitions primarily between the aqueous and interfacial regions, whereas α -tocopherol (TOC, vitamin E, Chart 1) is hydrophobic and water-insoluble and primarily partitions between the oil and interfacial regions. Figure 4 shows that both $\%CA_I^{33}$ and $\%TOC_I^{32}$ increase in the interfacial region with increasing Φ_I such that at surfactant $\Phi_I = 3.5$ to 4% more than 70% of both AO_Is are located in the interfacial region. Note that $\%CA_I$ increases from 70% in the interfacial region (30% in the aqueous) at $\Phi_I = 0.005$ up to 90% at $\Phi_I = 0.04$ (Figure 4). However, $\%TOC_I$ increases from ~20% in the interfacial region (80% in the oil) to 70% over the same region in the Φ_I range. This larger change in $\%AO_I$ when the initial $\%AO_I$ values are low makes sense because more AO can be transferred when the initial amount in the interfacial region is lower and because the upper limit on the amount of an AO in the interfacial region cannot exceed 100%.

Significantly, an increase in $\%AO_I$ with increasing Φ_I is not the same as an increase in interfacial AO_I molarity with increasing Φ_I . As the surfactant volume fraction increases, more AO is transferred from the oil or water regions into the interfacial region, but the interfacial molarity of AO_I is defined as moles of AO_I per liter of interfacial volume. Thus, if the interfacial volume increases faster than the rate of transfer of AO to the interfacial region, then both the AO_I molarity and k_{obs} will decrease with added surfactant (eq 7), which is what is generally observed.⁹ Typically, measured partition constants are often large, $\geq 10^2$, and often 50% or more of the AO is in the interfacial region at the lowest surfactant volume fraction used. Consequently, the dilution of AO_I increases more rapidly than the transfer of AO to the interfacial region and k_{obs} decreases (Figure S3, Supporting Information). Stated differently, the interfacial region is a better solvent for AOs that are composed of polar and hydrocarbon groups than bulk oil or water regions. For example, the results in Figure 4B,D show that at any given Φ_I a change in the oil to water ratio does not have a large effect on $\%AO_I$. For instance, at $\Phi_I = 0.005$, $\%CA_I$ decreases less than 10% upon changing the oil to water ratio from 2:3 to 1:9 (a 4-fold decrease in the amount of oil relative to water). Similar changes were observed for $\%TOC_I$ (Figure 4D) at the same Φ_I , although sensibly the order is reversed (i.e., $\%TOC_I$ increases about 2-fold with a 2-fold decrease the amount of oil relative to water).

The k_I values in Table 1 suggest a correlation of surfactant HLB and k_I in the emulsions for the AOs listed. The variation of k_I values with emulsions prepared with Tweens (HLB 16.7–15) suggests that the AOs in Table 1 experience a similar environment because the k_I values are very similar. However, in emulsions prepared with the more hydrophobic Spans (HLB 1.8–8.6; esters of sorbitan and long-chain carboxylic acids), the k_I values are significantly lower, decreasing by a factor of 2 to 3 with respect to the values in Tween emulsions.³² Such differences indicate that AOs are reacting in interfacial regions with different properties, e.g., lower polarity, which might be expected because the headgroup region of Tween 20 has three polyoxyethylene chains per sorbitan group per tail, whereas Span 20 has an alkyl tail and –OH groups but no polyoxyethylene groups (Chart 1).

Trends in P_W^I and P_O^I values with surfactant HLB (Table 1) show that they depend on the AO type. P_W^I values for hydrophilic gallic acid (GA, pH 3.6) do not depend on surfactant HLB

(Table 1, row 7), but for the more hydrophobic propyl gallate (PG), both P_W^I and P_O^I values increase with increasing surfactant HLB (Table 1, row 8), contrary to the observed decrease in the P_O^I values for the much more hydrophobic TOC (Table 1, row 11).

Figure 5³² shows the effect of surfactant HLB on %AO in the interfacial region of emulsions. %AO_I values were obtained by

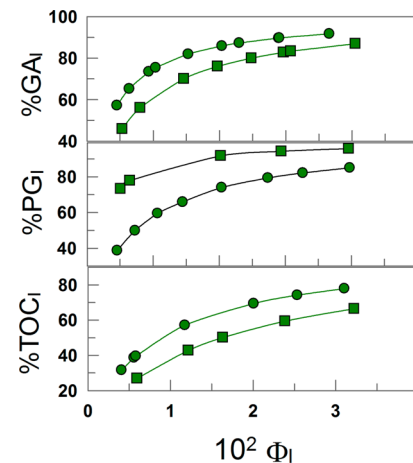


Figure 5. Effect of surfactant HLB on the distribution of GA, PG, and TOC in stripped corn oil emulsions. (Green ●) HLB 16.7 (Tween 20) and (green ■) HLB 10.6 (blend 25.2% Tween 20 + 74.8% Tween 80). (Reproduced with permission from Elsevier and *J. Colloid Interface Sci.*; see ref 32.).

employing the partition constant values in Table 1, rows 7, 8, and 11 (section S.5.2, Supporting Information). The fraction of GA in the interfacial region depends on the particular surfactant volume fraction. For Φ_I values >0.04 , %GA_I extrapolates to ~100%, indicating that GA may associate completely with the interfacial region of the emulsions. PG is significantly more hydrophobic and less soluble in water than GA because of the acylation of the carboxylic group. At the lower surfactant HLB, the %PG_I is higher, indicating that when surfactant HLB is lower, the solubility of PG is higher in the interfacial region. TOC is water-insoluble and much more hydrophobic than GA or PG, and at the lowest Φ_I investigated (0.004), the percentage of TOC in the interfacial region decreases from 30% (HLB = 16.7, Tween 20) to 20% (HLB = 8, Span 20); this decrease is much greater at higher Φ_I values.

Taken together, these distribution results clearly show that changing the surfactant HLB correlates with a modest effect on the distribution of moderate- to high-hydrophobicity AOs and a much smaller effect on the distribution of hydrophilic AOs. The results in Figure 5 suggest that the percentage of AOs in the interfacial region of the emulsions does not correlate directly with the polarity of the AO as measured by its HLB because the percentage of GA and PG in the interfacial region is higher than that of TOC. Note that GA and PG are primarily distributed between the aqueous interfacial regions of the emulsions but TOC is distributed between the oil and interfacial regions.

IVc. Effects of Acidity. Dietary AOs include ascorbate, tocopherols, carotenoids, and a large variety of bioactive plant phenols.³¹ They are generally uncharged polar organic molecules that have variable oil and water solubility. The first ionization of a phenolic –OH (multiple –OH groups are possible) on the aromatic moiety is about $pK_a \approx 8\text{--}10$. At the typical acidities of emulsified foods (pH range 2–6),³⁴ the –OH groups are not

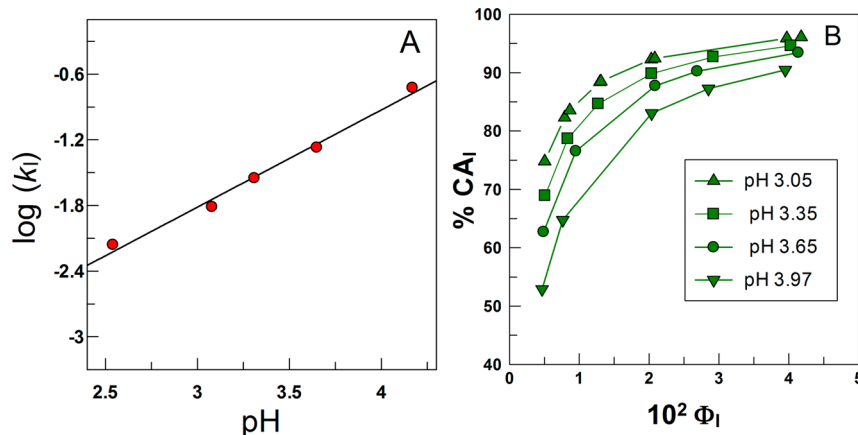


Figure 6. (A) log pH plot for the variation of the interfacial rate constant k_i for the reaction between 16-ArN₂⁺ and gallic acid (ref 36). (B) Variation in the percentage of caffeic acid, %CA_i, between pH 3 and pH 4 (ref 53). Detailed experimental conditions for these results are available in the indicated references above.

significantly deprotonated. However, the carboxylic groups present on some AOs may be partially ionized in acidic emulsions because their acidity constants, pK_a , range from 4.1 to 4.5.^{55,56} Consequently, their solubilities in the aqueous region increase significantly when the emulsion acidity is decreased (pH increased) because anionic AOs are poorly soluble in oils but much more soluble in water than their protonated forms. Thus, the charge on phenolic acids may range from 0 to -1 in food emulsions, and a change in emulsion acidity has a significant effect on the AO distribution among the oil, interfacial, and water regions.^{32,34,37} Nonaromatic AOs such as ascorbic acid (vitamin C, $pK_a = 4.2$)⁵⁷ may also be partially ionized in acidic foods.

To date, our partitioning experiments show that both P_W^I and k_i values depend upon the solution acidity.^{8,36,53} Figure 6 contains unpublished results. Figure 6A illustrates the linear dependence of $\log k_i$ on pH for the reaction of gallic acid with 16-ArN₂⁺, consistent with the deprotonated phenol as the reactive form of gallic acid and with the proposed mechanism for the reaction between 16-ArN₂⁺ and TBHQ (Scheme 2).

The effect of the ionization of a carboxylic acid group on an AO on k_{obs} for its reaction with 16-ArN₂⁺ is reflected in a decrease in P_W^I with decreasing aqueous acidity. To a first approximation, the pK_a of AO in water is the same as in the emulsion interface, $pK_a(w) \approx pK_a(I)$,¹⁴ because interfacial regions of nonionic micelles have smaller effects on the pK_a values of weak acids than those of ionic micelles that may change the pK_a of an acid 1 to 2 pK_a units.¹⁴ At low acidities ($pH \ll pK_a$), the carboxylic acid groups on AO in aqueous solution are protonated, and their P_W^I values should be independent of increasing acidity. Conversely, at $pH > 6$, an AO carboxylic acid group should be fully ionized, which would significantly reduce the incorporation of the AO into the interfacial region of an emulsion because of its increased solubility in the aqueous region compared to its neutral form. Thus, a change in the acidity of an emulsion between pH 2 and 6 has little effect on the ionization of a phenolic -OH group of an AO because its pK_a values are ~8–10, at pH ≤ 6 it is only weakly ionized ($\leq 1\%$), and its P_W^I value is determined by the neutral form.

Two other points should be mentioned: (a) The reaction rate of 16-ArN₂⁺ with the phenolic anion of an AO is near the diffusion-controlled limit,⁴⁹ and only at extremely low concentrations of the anionic form does the 16-ArN₂⁺ reaction proceed at a measurable rate on an ordinary spectrometer. (b) If an AO is functionalized with a carboxylate group and a

hydrophobic group, then it may become ionic and surfactant-like or a hydrotrope and associate with emulsion interfacial regions like a surfactant. Literature reports indicate that phenoxide and arylcarboxylate ions do not incorporate appreciably into nonionic micelles but more hydrophobic anionic AOs do.^{58–60} Consequently, P_W^I values of AOs measured at a single pH or proton concentration that contain one (or more) carboxylic acid groups such as GA and CA must be considered to be apparent values because their distributions between the aqueous and interfacial regions depend on acidity.

Figure 6B shows the effects of aqueous acidity on the percentage of caffeic acid ($pK_a(1) = 4.62$) in the interfacial region of 1:9 corn oil emulsions. At any acidity, %AO_I increases upon increasing Φ_I from $\%CA_I \approx 50$ ($\Phi_I = 0.005$, pH 3.97) to $\%CA_I \approx 90$ at the same pH and $\Phi_I = 0.04$. At any given Φ_I , a decrease in pH leads to a significant (low Φ_I) to measurable (high Φ_I) increase in %AO_I. Because the first ionization of most phenolic acids is that of a carboxylic acid group, they should have similar pK_a values in acidic solution and similar variations of %AO_I with acidity to those shown in Figure 6B.

IVd. Effect of Surface Charge and Cationic, Anionic, and Zwitterionic Surfactants. Recent results show that the pseudophase model also works in emulsions of both cationic and anionic surfactants and provides reasonable estimates of the partition constants of TBHQ in emulsions composed of medium-chain-length triglycerides (MCT) in both cationic (CTAB) and anionic (SDS) emulsions.⁶¹ To monitor the reaction on a human time scale, e.g., minutes, by the dye derivatization method, the solution acidity had to be changed considerably from one that works in a nonionic emulsion, ca. pH 3. In CTAB emulsions, the pH was lowered to about 1.5 by adding HBr. In SDS emulsions, it was raised to about 5.7 by adding acetate buffer, an ~4 pH unit increase from CTAB emulsions. These requirements fit the well-known observations that the interfacial acid concentrations are lower in cationic and higher in anionic micelles than in the surrounding aqueous solution.¹⁴ Hydronium ions are counterions to anionic surfaces, and the interfacial H₃O⁺ concentration is greater than the bulk concentration when acid is added. Whereas hydronium ions are co-ions for cationic interfaces, their local concentrations are lower in the interfacial regions of cationic surfactants and the interfacial region has a higher concentration of OH⁻ than in the bulk solution. The addition of NaBr to both emulsions increased k_{obs} in SDS emulsions and decreased k_{obs} in CTAB emulsions,

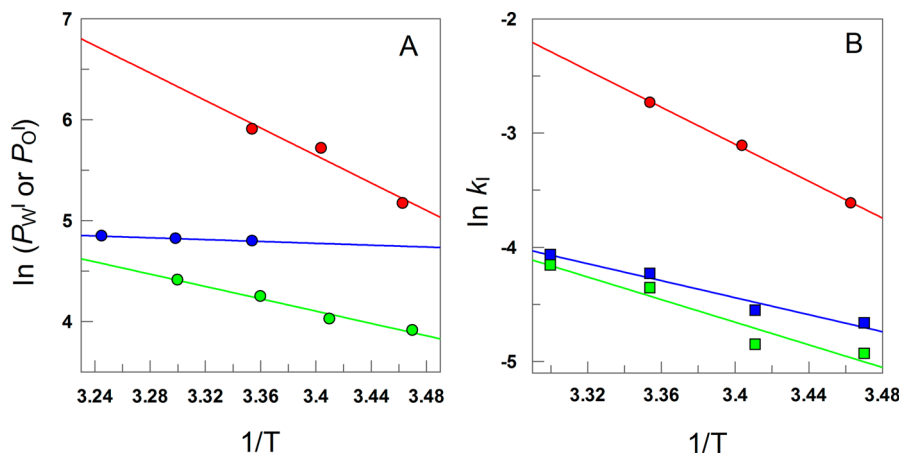


Figure 7. (A) Illustrative plot of the variation of partition constants P_W^I (catechin, red ●; gallic acid, blue ●) (refs 66 and 36) and P_O^I (α -tocopherol, green ●) (ref 67) at a series of temperatures. (B) Representative Arrhenius plots for the variation of the interfacial rate constants k_I for the reaction between 16-ArN_2^+ and catechin (red ●), α -tocopherol in 1:1 (blue ■) and 1:4 (green ■) octane emulsions. Detailed experimental conditions for these results are available in the indicated references.

consistent with the treatment of emulsion surfaces as ion exchangers. (See Supporting Information, section S6, Figure S4.) Added Br^- increases interfacial H_3O^+ at cationic surfaces by Donnan equilibrium⁶² and reduces k_{obs} . Added Na^+ displaces H_3O^+ from SDS interfaces by ion exchange,^{10,14} thus reducing interfacial acidity and increasing k_{obs} .

Specific anions also influence the interfacial acidity of zwitterionic surfactant *N*-tetradecyl-*N,N*-dimethylammonio-1-propanesulfonate, SB3-14. Added anions decrease k_{obs} for the reaction of 16-ArN_2^+ with TBHQ in SB3-14. Zeta potential measurements by Nome and co-workers show that zwitterionic micelles become negatively charged in the presence of added salt;⁶³ i.e., anions associate more strongly to the zwitterionic interface than do cations. The zeta potential increase follows a Hofmeister series. Larger, more polarizable anions associate more strongly with the zwitterionic interface than smaller, more strongly hydrated anions. (See Supporting Information, section S7, Figure S5.) The excess interfacial anions give the interfacial region a negative charge that attracts cations as counterions, including H_3O^+ , and makes the interfacial acidity greater than the bulk acidity. An increase in interfacial acidity enhances the protonation of TBHQ and slows the reaction with interfacial 16-ArN_2^+ , as observed.

IVe. Effect of Droplet Size. Recent unpublished results⁶⁴ support our contention that rate constants for reactions in emulsions of different sizes are insensitive to changes in droplet size in emulsions of constant composition. Emulsions were prepared by three mixing methods from high to low intensity, high-pressure homogenization, sonication, and magnetic stirring. Their size distributions were measured by static light scattering before and after measuring k_{obs} for the reaction of 16-ArN_2^+ with TBHQ at 25 °C. The homogenized emulsion gave a narrow, nearly Gaussian distribution of sizes, 0.06–0.2 μm, but wider distribution ranges were obtained for emulsions prepared by sonication, 0.05–1.2 μm, and magnetic stirring, 1–25 μm. The values of k_{obs} are 1.4×10^{-2} , 0.8×10^{-2} , and $0.7 \times 10^{-2} \text{ s}^{-1}$, respectively, and the maximum variation is only a factor of 2. These results are completely consistent with the idea that the polarity of the interfacial region is insensitive to droplet size and that the medium properties of the interfacial region are essentially constant.

IVf. Effects of Temperature: Thermodynamic Parameters for the Transfer of AOs between Regions and Activation Parameters for the Reaction in the Interfacial Region of the Emulsions. The effects of heating on the chemistry of lipid oxidation are complex because lipids are generally present in foods as oil-in-water emulsions and multiple changes occur simultaneously with increasing temperature,⁶⁵ including increasing the rates of the chemical reactions^{9,31} and altering reactant distributions among the oil, interfacial, and aqueous regions of the emulsion.^{36,53,66,67}

We investigated the effects of temperature on the distributions of AOs that have negligible oil solubility (caffeic and gallic acids, catechin),^{36,53,66} and negligible water solubility of α -tocopherol (TOC).⁶⁷ Increasing the temperature from $T = 15$ to 35 °C has small effects on AO distributions. Changes in %AO_I with T show the same trend for catechin (CAT) and for TOC, increasing from %TOC_I = 60 at $T = 15$ to %TOC_I = 70 at $T = 35$ °C. However, a similar increase in T has only a moderate effect on the distributions of CA and GA, decreasing %GA_I ≈ 42 ($T = 15$) to %GA_I ≈ 38 at $T = 35$ °C.⁶⁶

Values of P_W^I and P_O^I obtained at a series of temperatures were used to estimate the free energy, $\Delta G_T^{0,W \rightarrow I}$, enthalpy, $\Delta H_T^{0,W \rightarrow I}$, and entropy, $\Delta S_T^{0,W \rightarrow I}$, of transfer of AOs from the aqueous to the interfacial and from the oil to the interfacial regions of emulsions. Details and the derivation of the relevant equations are given elsewhere.⁹ Values of the Gibbs free energy/mole for the transfer of AO from the aqueous or the oil to the interfacial region, $\Delta G_T^{0,W \rightarrow I}$ and $\Delta G_T^{0,O \rightarrow I}$, respectively, are given by eqs 9 and 10, where V_m^O , V_m^W , and V_m^I are the molar volumes of oil, water, and surfactant, whose values can be obtained from literature density values and are assumed to be constant over the temperature ranges commonly employed ($T = 290$ –310 K) in partitioning studies.⁶⁸

$$\Delta G_T^{0,W \rightarrow I} = \mu_{AO}^{0,I} - \mu_{AO}^{0,W} = RT \ln \frac{V_m^W}{P_W^I V_m^I} \quad (9)$$

$$\Delta G_T^{0,O \rightarrow I} = \mu_{AO}^{0,I} - \mu_{AO}^{0,O} = RT \ln \frac{V_m^O}{P_O^I V_m^I} \quad (10)$$

Both the enthalpy and entropy of transfer of AO between the aqueous and interfacial regions in emulsions can be obtained by

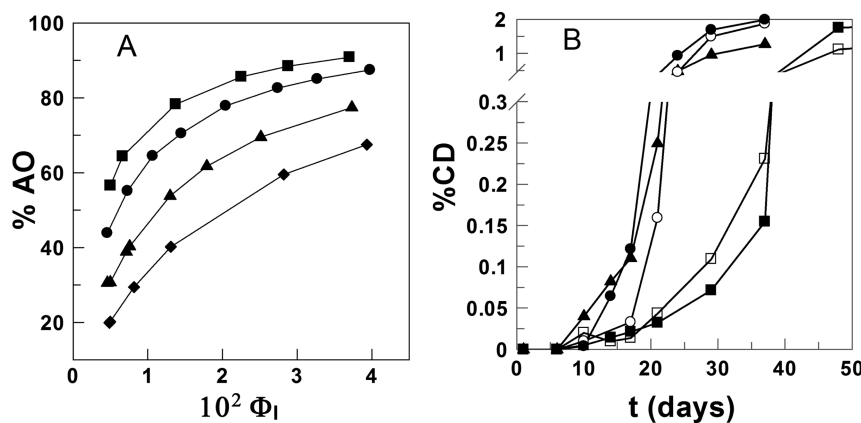


Figure 8. (A) Percent AO in the interfacial region of a 3:7 olive oil/Tween20/acidic water (pH 3.7) emulsion at 25 °C. (■) PG, (●) GA, (▲) OG, and (◆) LG. (B) Variation of the percentage of conjugated dienes with time (3:7 olive oil emulsions stabilized with 1% Tween 20). The oxidative stability is determined by the time required for the formation of 0.1% conjugated dienes (%CD). (▲) Control, (●) LG, (○) OG, (■) PG, and (□) GA. [AO] ≈ 3.3×10^{-4} M, T = 45 °C. Detailed experimental conditions for these results are available in refs 34 and 69.

using the van't Hoff equation (eq 11) and the Gibbs equation (eq 12), respectively. Figure 7^{36,66,67} shows the variations of $P_W^{I_1}$ and $P_O^{I_1}$ (7A) and k_I (7B) for a series of temperatures.

$$\Delta H_T^{0,W \rightarrow I} = R \left[\frac{\partial (\ln P_W^{I_1})}{\partial (1/T)} \right]_p \quad (11)$$

$$\Delta G_T^{0,W \rightarrow I} = \Delta H_T^{0,W \rightarrow I} - T \Delta S_T^{0,W \rightarrow I} \quad (12)$$

The activation energy (E_a) and the activation parameters (ΔH^\ddagger and ΔS^\ddagger) for the reaction between 16-ArN₂⁺ and the AOs in the interfacial region of the emulsion were estimated from the variation of k_I with T by using the Arrhenius equation. Figure 7B illustrates the determination of the activation energies for the reaction between 16-ArN₂⁺ and AOs of different hydrophobicities.

We found that the free energies of transfer of hydrophobic TOC⁶⁷ and hydrophilic GA³⁶ and CAT⁶⁶ (Chart 1) are negative at all temperatures, consistent with our earlier observation at constant temperature. TOC is composed of a long hydrophobic phytyl chain attached to a more hydrophilic chromanol ring (Chart 1). In the oil region, TOC is surrounded by low-polarity molecules (octane), but in the interfacial region, it is probably oriented with its chromanol group in contact with the surfactant headgroups and water and the tail in contact with oil. We expected enthalpic stabilization of the chromanol, but surprisingly, the free energy of transfer proved to be entropy-driven because the large, positive enthalpy term was overwhelmed by an even larger and more negative $-T \Delta S_T^{0,W \rightarrow I}$ term.⁶⁷ Gallic acid, unlike TOC, is a polar phenolic AO containing four acidic groups, three phenolic -OHs, and one carboxylic acid. Its entropy of transfer from the aqueous to the interfacial region is large and positive and the enthalpy of transfer is small and negative, so the transfer of gallic acid from the aqueous to the interfacial region is also primarily entropy-driven and is accompanied by a net increase in the disorder. CAT (Chart 1) contains two aromatic rings that are bound together by three carbon atoms forming a flat oxygenated heterocycle. The transfer of CAT is enthalpy-driven because the transfer process of CAT from the aqueous to the interfacial region is strongly exothermic and it is only partially balanced by a negative (decrease in) entropy.⁶⁶

Together these results suggest that the thermodynamic driving forces for the transfer of AOs from the aqueous and oil regions to the interfacial region are different. A decrease in enthalpy for the transfer of an AO from the aqueous to the interfacial (or from the oil to the interfacial) region of emulsions indicates stronger interaction energies, e.g., a net increase in hydrogen bonding or a net increase in the hydration of the AO by water, but an increase in entropy suggests an increase in molecular disorder caused by a less-ordered association of the AO with the water and headgroups in the interfacial region compared to bulk water. However, because of the experimental difficulties in determining variations of the partition constants with temperature and because the number of transfer enthalpy and entropy experiments of AOs completed to date is small, our conclusions should be considered tentative.

V. EFFECT OF AO HYDROPHILIC–LIPOPHILIC BALANCE (HLB) ON AO EFFICIENCY

Va. Cut-Off Effect. In recent times, several groups have reported multiple examples of maxima in bulk AO efficiency with increasing alkyl tail length on esters of AOs from 1 to 20 carbons. A maximum in AO efficiency occurs at intermediate chain lengths from 6 to 12 carbons.¹² These maxima appear to be a general characteristic of AO hydrophobicity because it has been observed with different AOs¹² including chlorogenates, hydroxytyrosols, rosmarinates, and gallate esters (Chart 1). The marked decrease in AO efficiency at longer chain lengths is called the cut-off effect because it suggests a “collapse” in AO efficiency.¹² Three explanations have been proposed for the effect of increasing AO hydrophobicity on its efficiency: (a) the reaction is slowed by a decrease in AO diffusivity with increasing AO hydrophobicity; (b) a larger fraction of the more hydrophobic AOs are dissolved in the hydrophobic regions of the aggregates and unavailable for reaction; and (c) the AOs are sequestered in separate aggregates.¹²

In 2013 and 2015, we reported maxima in AO efficiency in nonionic emulsions for two different AOs and their esters of various chain lengths (Chart 1) gallic and caffeic acids and their alkyl esters.^{34,69} We used the chemical kinetic method to determine $P_O^{I_1}$ and $P_W^{I_1}$ of the acids and alkyl esters of these AOs. The results show that with increasing alkyl chain length $P_W^{I_1}$ increases, $P_O^{I_1}$ and %AO_I go through maxima with increasing chain length, and these maxima match the maximum in the

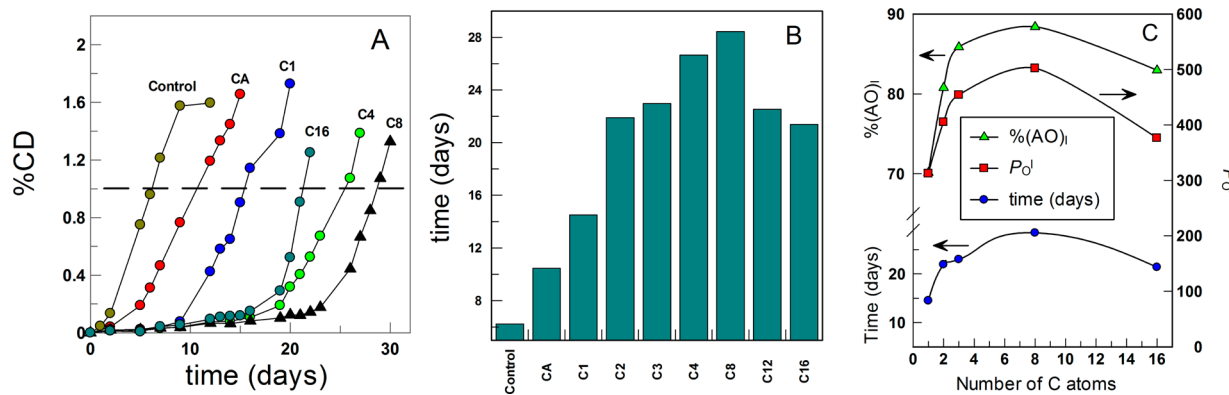


Figure 9. (A) AO efficiency of caffeic acid derivatives in 4:6 olive oil:water emulsions at 1% tween 20 volume fraction as determined by the variation in the formation of conjugated dienes with time at 60 °C. The dashed line marks the days required for the increase of 1% in the conjugated dienes content. (B) Replot of panel A showing the effect of AO chain length (hydrophobicity) on time required to increase the conjugated dienes content 1.0%. The control sample in A and B contains no added AO. (C) Variations of the time required to reach 1% conjugated dienes and of values of P_O^I and $\%AO_I$ with the number of C atoms in the alkyl chain of caffeic acid esters. Note that all three curves have similar profiles and that the maxima occur at about eight carbon atoms for all three. Detailed experimental conditions for these results are available in ref 69.

Table 2. Values of P_W^I , P_O^I , and k_I for (Left) GA, PG, OG, and LG with Various Oils in Different Oil/Water Ratios^a and (Right) for CA, C₁, C₂, C₃, C₈, and C₁₆ in 3:7 Olive Oil/Water and 1:9 Corn Oil/Water Emulsions^b

AO	emulsion	o/w	P_W^I	P_O^I	$10^2 k_I (M^{-1} s^{-1})$	AO ^b	P_W^I	P_O^I	$10^2 k_I (M^{-1} s^{-1})$
GA	corn	1:4	131	5.59	5.59	CA	349	312	0.011
GA	corn	1:9	119	5.42	5.30	C ₁	720	405	0.011
GA	olive	3:7	101	5.30	5.30	C ₂	(3156)	454	0.016
PG	corn	1:9	204	242	14.0	C ₃	449	502	0.011
PG	olive	3:7	328	14.2	29.8	C ₈	58.0	376	0.014
OG	corn	1:1	29.8	26.5	36.6	C ₁₆	19.4	16.5	0.015
OG	corn	3:7	328	31.6	31.6		17.2	59.0	
LG	corn	1:1	19.4	58.0	56.0				
LG	corn	3:7	16.5	56.0	59.0				
LG	olive	3:7	17.2	59.0					

^aGA, gallic acid; PG, propyl gallate; OG, octyl gallate; and LG, lauryl gallate. ^bCA, caffeic acid; C₁, methyl caffeate; C₂, ethyl caffeate; C₃, propyl caffeate; C₈, octyl caffeate; and C₁₆, hexadecyl caffeate.

measured AO efficiency (Figure 8A,B). Note that in Figure 8A propyl gallate (PG) has the highest percentage in the interfacial region, and in Figure 8B it slows oxidation to the greatest extent (compare curves at 0.1% CD, conjugated dienes).

Figure 9 shows a similar set of results for caffeic acid and some of its esters,⁶⁹ although the data is represented differently. Figure 9A,B shows the bulk efficiency results, but this time the greatest efficiency is for the octyl gallate, OG. Figure 9C shows that the time required to reach 1% dienes, the percentage of the esters in the interfacial region, and P_O^I for the esters all reach maxima at OG.

The similarities of the shapes and efficiencies for GA, CA, and their esters are no mere coincidence but a natural consequence of the properties of emulsions and microemulsions at dynamic equilibrium as described by the pseudophase model. An AO that dissolves completely in the water or oil regions does not react or reacts very slowly because the concentration of 16-ArN₂⁺ in these regions is very small (eq 4). Because AO diffusion is orders of magnitude faster than its reaction with 16-ArN₂⁺ and because the stoichiometric AO concentration is present in large excess, the concentration of the AO in the interfacial region is constant throughout the time course of the reaction. The rate at which AO reacts with 16-ArN₂⁺ in the interfacial region depends on the fraction of AO in the region and its volume, i.e., the AO concentration in mol/L of interfacial volume. The molarity of the probe, 16-ArN₂⁺, at any time also depends on the interfacial

volume, but this change in molarity does not affect the measured value of k_{obs} or the calculated value of k_I .

Vb. Gallates in Olive and Corn Oil Emulsions with Tween 20. Table 2 shows the effect of increasing hydrophobicity of gallic acid esters (from 3 to 12 carbons) on P_W^I and P_O^I in corn and olive oils.³⁴ See the reference for details. Note that oil type and oil/water ratios have only a small effect on the P_W^I and P_O^I ratios.

As the alkyl chain length of the gallate esters increases, both P_W^I and P_O^I increase up to a maximum after which a further increase in gallate hydrophobicity results in a decrease in P_O^I and overall a shift in the distribution of the gallic acid esters from the aqueous to the interfacial to the oil regions with increasing ester chain length. The maxima in P_W^I and P_O^I values are for PG. We have found that when P_W^I and P_O^I values are on the order of 10^3 or greater, the amount of AO in the aqueous or oil phases becomes too small to measure precisely and we either do not report those numbers or show them as tentative within parentheses, e.g., P_O^I for GA (which has a low solubility in oil) and P_W^I for OG and LG, which have low solubilities in water. We do not know why k_I increases with chain length, but note that the two or three values for each AO are essentially the same and independent of oil type and the oil/water ratio. The results for caffeic acid esters are different, however (see below).

Figure 8A shows the increase in percent gallate derivative, $\%AO_I$, in the interfacial region with increasing Φ_I (Tween 20) for

the emulsions listed in Table 2 and calculated from equations s13 to s16 in the Supporting Information. The %AO_I decreases in the order PG > GA > OG > LG at all Φ_I and is consistent with the order of the partition constants. Figure 8B shows the effect of the same gallate AOs on the oxidative stability of olive oil as measured by the percent increase in the amount of conjugated dienes (CD) over a period of days. At 0.1% CD, the order of efficiency is the same as the %gallate in the interfacial region in Figure 8A.

Vc. Caffeates in Olive Oil/Water/Tween 20 Emulsions.

Table 2 also contains the results from chemical kinetics measurements for the reactions of a series of caffeic acid and caffeate esters in 2:3 olive oil/water having 1, 2, 3, 8, and 16 carbons in the alkyl tail, in which the last has the same length as the arenediazonium ion tail.⁶⁹ Details on the experimental conditions are in the reference. The partition and rate constants were obtained the same way as for the gallate derivatives. Each P_W^O value obtained in the absence of surfactant is from duplicate or triplicate measurements with deviations of $\leq 5\%$. The value of P_W^O between water and olive oil increases by about 10^4 from C₁ to C₁₆ carbon tail (not shown). The P_W^I and P_O^I values for gallate and caffeate esters show the same basic trend with increasing alkyl chain length, but the extent of the change is different. Unlike the gallate esters in Table 2, the P_W^I values increase significantly for the caffeates in olive oil, although the value for C2 is greater than 3000 and may not be accurate. However, the P_O^I values increase gradually and decrease for C₁₆.

The most striking difference for the two data sets is the absence of a trend in k_I values with increasing chain length of the caffeate esters, unlike the gallate k_I values that increase significantly with ester chain length. The reasons for the differences in k_I values for these two AOs are not known, but might have to do with changes in the interfacial position of the reactive phenolic group of the gallate esters with chain length. Nevertheless, the fundamental observation remains for both AOs: the %AO_I, the P_O^I , and also the AO efficiencies show maxima with increasing chain length (Table 2 and Figures 8 and 9).

VI. CONCLUSIONS

We emphasize that the combined chemical kinetic method and pseudophase kinetic model are grounded in thermodynamics and have worked successfully in homogeneous solutions of micelles and vesicles and in microemulsions and now in intact emulsions. The approach provides quantitative estimates of AO partition constants and distributions between water and interfacial and oil and interfacial regions and an estimate of the second-order rate constant in the interfacial region, k_I . The results are interpreted by applying a pseudophase kinetic model to the oxidation/reduction reactions of AOs with a specially designed hydrophobic arenediazonium ion and by assuming that the aggregate structure—continuous reaction region duality holds.

The physical impossibility of separating the interfacial region from the oil and aqueous regions of emulsions without disrupting the existing equilibria between oil, interfacial and aqueous regions within emulsions drove us to develop a new approach based on the structural similarities of microemulsions and emulsions, including that the reactants in both are in dynamic equilibrium and that the same chemical probe works in both systems.

The chemical kinetic method was used to estimate partition constants as a function of (a) AO structure, (b) oil type, (c)

acidity and surfactant charge and to demonstrate the independence of the rate constant on droplets size; (d) specific ion effects on the reaction in zwitterionic emulsions; and (e) estimated thermodynamic parameters for AO transfer between regions. Results with gallate and caffeate esters of variable alkyl chain length and hydrophobicity show that maxima observed for bulk-phase measurements of AO efficiencies with increasing chain length are also observed in determinations of the %AO_I and in P_O^I as obtained from the chemical kinetic method. The maxima with increasing alkyl group chain length (i.e., hydrophobicity) are a natural consequence of the shifting of the distributions of AOs from the interfacial to oil region based on their increasing oil solubility, and this shift is consistent with the logic of the pseudophase model.

VII. PERSPECTIVES AND PROSPECTS

The results open up the possibility of developing new approaches to obtaining a deeper understanding of mechanisms of lipid peroxidation in opaque emulsions and developing guidelines for selecting the most efficient AO for a particular application. The chemical kinetic method can be applied under a range of experimental conditions to obtain information on the various factors determining AO distributions in model food emulsions and the relationship of bulk AO efficiency to inhibiting lipid oxidation. This work is far from finished, and innovative strategies aimed at providing a full understanding of lipid oxidation and minimizing its impact are needed.

VIIa. Effects of the Interfacial Region on Lipid Oxidation. The chemical kinetic method provides a robust technique for determining AO partition constants and distributions over wide ranges of solution composition, and the approach provides information on how the AO efficiency depends on both the intrinsic chemical reactivity of the AO and its concentration in the reaction region. However, the detailed oxidation mechanism within the interfacial region, including the mechanisms of the participating reactions and the locations of radical initiators, still needs to be determined.^{3,5,6}

VIIb. Prooxidant and Synergistic Effects. Under certain experimental conditions, AOs are reported to behave as prooxidants at higher concentrations or show synergistic activity for certain combinations of antioxidants.⁶ The prooxidant activity is apparently related to the metal-catalyzed oxidation of polyphenols and reaction conditions such as pH, temperature, and oxygen concentration. The chemical kinetic method should provide quantitative information on the concentrations and distributions of AOs under conditions in which prooxidation and synergistic effects are observed.

VIIc. Interfacial Charge Effects. Some AOs and other components, including emulsifiers used in emulsion preparation, are charged, including small-molecule emulsifiers and also proteins that may be neutral, anionic, cationic, or zwitterionic, depending upon pH. The distributions and reactivity of AOs in ionic emulsions may show complex dependencies on interfacial charge, pH, and the type and concentration of added salts, including metal ions and anions. For example, many AOs have carboxylic acid functional groups, e.g., Trolox, and their distributions will depend on the charge of the emulsifier used and solution pH. When an AO's distribution between the aqueous and interfacial regions depends on the emulsifier charge at relatively high pH, its distribution may also depend on the ionic strength and counterion type (section IVd).

In principle, the same approaches that successfully describe ion distributions in association colloids using pseudophase models

with the interfaces acting as selective ion exchangers¹⁰ should work with emulsions of ionic surfactants. Both cationic and zwitterionic micellar interfaces selectively bind anions, and the ion binding order typically follows the Hofmeister series (section IVd). The observation of ion-specific effects means that a careful selection of salts added to ionic or zwitterionic emulsions should permit the fine-tuning of emulsion properties for particular applications. The high local concentrations of cationic head-groups will induce the selective association of anions, and the converse is true for cations at anionic interfaces. The local concentrations of counterions may be 1 to 2 orders of magnitude greater than their concentration in the bulk. Co-ion concentrations, on the contrary, should be reduced by similar amounts. The effect of nonreactive counterions on interfacial concentrations of reactive counterions, e.g., nonreactive Na^+ and H^+ at anionic surfaces or nonreactive Br^- and OH^- at cationic surfaces, can be described by ion-exchange constants, whereas the effect of co-ions on reactive counterions can be described by an empirical Donnan equilibrium constant, e.g., between H^+ and the X^- ions at cationic surfaces, section IVd.

VIIId. Challenges in the Food and Pharmaceutical Industries. Much still needs to be done in areas such as pharmacy, medicine, biology, and so forth where emulsions are widely employed in, for example, the optimization of drug distributions, drug delivery, and parenteral nutrition. Present food challenges include the development of edible delivery systems to encapsulate, protect, and release bioactive and functional lipophilic constituents (e.g., ω -3 lipids). Each of these delivery systems can be produced from food-grade ingredients (e.g., lipids, proteins, polysaccharides, surfactants, and minerals) and can be used for a number of purposes such as control of the lipid bioavailability, targeting the delivery of bioactive components within the gastrointestinal tract, and the design of food matrices that delay lipid digestion. Finding the appropriate delivery systems and assessing the concentration, reactivity, and physical stability of the AOs is especially challenging for the food industry because it is limited to the use of edible ingredients that can be used as stabilization materials.

■ ASSOCIATED CONTENT

Supporting Information

Discrete structures. Assumptions of the pseudophase model as applied to reactions in microemulsions and emulsions. Dye Derivatization and linear sweep voltammetry methods. Derivations of expressions for k_{obs} versus Φ_L , partition constants P_O^{-1} and P_W^{-1} , and distributions of AOs in microemulsions and emulsions. Determination of partition constants and AO distributions. Effect of added NaBr on the reaction rate of TBHQ with 16-ArN₂⁺ in CTAB and SDS emulsions. Effect of added salts on the rate of reaction of TBHQ with 16-ArN₂⁺ in SB3-14 zwitterionic emulsions. This material is available free of charge via the Internet at <http://pubs.acs.org>.

■ AUTHOR INFORMATION

Corresponding Authors

*E-mail: cbraivo@uvigo.es. Phone: +34986812303. Fax: +34986812556.

*E-mail: romsted@rutchem.rutgers.edu. Phone: 848-445-3639. Fax: 732-445-5312.

Notes

The authors declare no competing financial interest.

Biographies



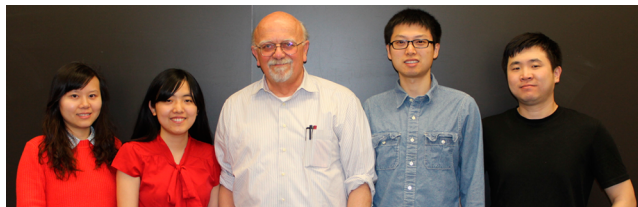
VIGO group (left to right): Verónica Sánchez-Paz, María José Pastoriza-Gallego, Sonia Losada-Barreiro, and Carlos Bravo-Díaz

Verónica Sánchez-Paz received her Ph.D. degree from University of Vigo in 2008 under the supervision of Professor Carlos Bravo-Díaz. In her thesis work, she developed batch methods to monitor dediazoniations in opaque emulsions to determine the distributions of antioxidants in a variety of oils. She is currently teaching chemistry at the high-school level in Vigo, Spain and continues collaborating with the Bravo research group.

Maria José Pastoriza received her Ph.D. degree from University of Vigo in 2006 under the supervision of Professor Carlos Bravo-Díaz. Her thesis work was on the development of electrochemical methods to monitor dediazoniations in emulsified systems. Currently she is working at the University of Minho at Guimaraes, Portugal, on the chemistries of carbon nanotubes and graphene.

Sonia Losada-Barreiro received her Ph.D. degree from University of Vigo in 2008 under the supervision of Professor Carlos Bravo-Díaz. She focused on the kinetics and mechanisms of the reactions between arenediazonium ions and antioxidants and the distribution of antioxidants in edible oils. She is currently working at the University of Porto, Portugal, developing omega-3 lipid-based functionalized foods.

Carlos Bravo-Díaz received his Ph.D. degree in 1991 under the supervision of Prof. Ramón-Leis- Fidalgo studying the effects of micellar systems on nitrosation reactions. He joined the Romsted group (1991–1993) and studied micellar effects on the Sandmeyer reaction. In 1993, he obtained a position as assistant professor at the University of Vigo, Spain, and is now a full professor. He has authored or coauthored more than 100 peer-reviewed papers and book chapters. His major research interests include solvolytic arenediazonium chemistry and the quantitative approach of physical organic chemistry to modeling chemical reactivity at aqueous interfaces.



Rutgers group (left to right): Qing Gu, Changyao Liu, Laurence Stuart Romsted, Xiang Gao, and Yongliang Zhang

Qing Gu obtained her B.S. degree in applied chemistry from Wuhan University, China, in 2006 and her M.S. degree in organic chemistry from University of Science and Technology of China in 2009. She is currently a Ph.D. candidate in Romsted's group in the department of chemistry and chemical biology at Rutgers University—New Brunswick. Her research is focused on investigating the distributions and activities of phenolic antioxidants in various aggregation systems using a chemical kinetic method.

Changyao Liu received her B.S. in chemistry from University of Science and Technology of China in 2011. She is currently a Ph.D. candidate in

Romsted's group in the department of chemistry and chemical biology at Rutgers University—New Brunswick. Her research focused on using the chemical trapping method to better understand the contributions of specific ion effects on the delicate balance of forces controlling the spontaneous self-assembly of association colloids.

Laurence (Larry) Stuart Romsted has been a member of the faculty of the chemistry and chemical biology department at Rutgers University—New Brunswick since 1980. He earned an A.B. degree (1964) at DePauw University, Greencastle Indiana, a Ph.D. degree (1975) with E. H. Cordes at Indiana University, Bloomington, and was a postdoctoral fellow with C. A. Bunton, University of California, Santa Barbara from 1976 to 1980. He is a physical organic chemist by training, and his research is on using probe methods to understand the delicate balance of forces controlling the spontaneous self-assembly and properties of association colloids, especially the ion-specific effects observed in the still incompletely understood Hofmeister series. His scientific contributions include the development of the pseudophase ion exchange model for rates and equilibria of reactions in association colloids; the creation of the chemical trapping method for estimating the interfacial molarities of weakly basic nucleophiles, including water, within the interfacial regions of surfactant aggregates; the chemical kinetic method for determining the partition constants of antioxidants between oil and interface and water and interfacial regions of emulsions; and recently the employment of the chemical trapping probe to determine the location and orientation of a peptide or protein within a membrane mimetic interfacial region by cleaving the interfacial amide bonds.

Xiang Gao earned his B.S. in chemistry from Kuang Yaming Honors School, Nanjing University, Jiangsu, China, in 2009. He then joined Romsted's group at Rutgers University—New Brunswick. His research focuses on the Hofmeister series at interfaces of micelles, emulsions, and oil/water mixtures. To study anion behavior at the interfaces of surfactant aggregates, he utilizes an arenediazonium ion-based chemical probe that is incorporated into the interfacial region and reacts specifically with weakly basic nucleophiles within that region. He also did an internship at the Schlumberger Doll Research Center focusing on viscoelastic surfactants.

Yongliang Zhang received his B.S. degree in pharmaceutical sciences from Tianjin University, China, in 2008. He is currently a Ph.D. candidate in the department of chemistry and chemical biology at Rutgers, the State University of New Jersey. His research is primarily focused on developing chemical and analytical approaches for determining the orientations and conformations of peptides at biomimetic interfaces.



Gunaseelan Krishnan received his M.Sc. degree in analytical chemistry and M.Phil in environmental chemistry from Andhra University, India, in 1991 and 1996, respectively. He received his Ph.D. in chemistry from

North-Eastern Hill University, India, in 2001. He was a postdoc at Rutgers for 8 years where he developed the electrochemical kinetic method and he and Romsted continue collaborating. His research interests include transport properties of micelles and microemulsions and in determining antioxidant distributions in emulsions by applying the pseudophase kinetic model.



Aijaz A. Dar earned his Ph.D. degree in 2008 from Jadavpur University, Kolkata, India and is presently working as an assistant professor in the department of chemistry, University of Kashmir, India. He worked as a UGC-Raman postdoctoral researcher at Rutgers University—New Brunswick from 2013 to 2014. His research interests include the exploration of self-assembled soft systems based on surfactants and polymers towards their prospective catalytic and transport properties. He has published over 45 scientific papers in this field.

ACKNOWLEDGMENTS

S.L.-B. and C.B.-D. gratefully acknowledge financial support from the following institutions: Xunta de Galicia (10TAL314003PR), Ministerio de Educación y Ciencia (CTQ2006-13969-BQU), and Universidad de Vigo. L.S.R., C.L., X.G., Q.G., and Y.Z. appreciate financial support by the National Science Foundation, grant no. CHE 0411990, and by Agriculture and Food Research Initiative Competitive, grant no. 2009-02403 from the USDA National Institute of Food and Agriculture. We also appreciate helpful discussions with Fred Menger on droplet size affects, and with Frank Quina on dynamic equilibrium and the Acree–Curtin–Hammett principle, and with Fátima Paiva-Martins for fruitful discussions on oil and food compositions and her invaluable contributions to the development of the bulk oxidation experiments. L.S.R. thanks Clifford Bunton for his unstinting support for decades.

REFERENCES

- (1) Moore, R. *Niels Bohr: The Man, His Science, and the World They Changed*; MIT Press: Cambridge, MA, 1985.
- (2) Porter, W. L. Paradoxical Behavior of Antioxidants in Foods and Biological Systems. *Toxicol. Ind. Health* **1993**, *9*, 93–122.
- (3) Schaich, K. M. Thinking Outside the Classical Chain Reaction Box of Lipid Oxidation. *Lipid Technol.* **2012**, *24*, 55–58.
- (4) Laguerre, M.; Lecomte, J.; Villeneuve, P. Evaluation of the Ability of Antioxidants to Counteract Lipid Oxidation: Existing Methods, New Trends and Challenges. *Prog. Lipid Res.* **2007**, *46*, 244–282.
- (5) Wanasyundara, P. K. J. P.; Shahidi, F. Antioxidants: Science, Technology, and Applications, In *Bailey's Industrial Oil and Fat Products*; Shahidi, F., Ed.; Wiley & Sons: New York, 2005; pp 431–489.
- (6) Zhong, Y.; Shahidi, F. Antioxidant Behavior in Bulk Oil: Limitations of the Polar Paradox Theory. *J. Agric. Food. Chem.* **2012**, *60*, 4–6.

- (7) Waraho, T.; McClements, D. J.; Decker, E. A. Mechanisms of Lipid Oxidation in Food Dispersions. *Trends Food Sci. Technol.* **2011**, *22*, 3–13.
- (8) Bravo-Diaz, C. Diazohydroxides, Diazoethers, and Related Species. In *Patai's Chemistry of the Functional Groups: The Chemistry of Hydroxylamines, Oximes, and Hydroxamic Acids*; Rappoport, Z., Lieberman, J. F., Eds.; Wiley & Sons: Chichester, U.K., 2011; Vol. 2, p 853.
- (9) Romsted, L. S.; Bravo-Diaz, C. Modeling Chemical Reactivity in Emulsions. *Curr. Opin. Colloid Interface Sci.* **2013**, *18*, 3–14.
- (10) Bunton, C. A.; Nome, F.; Quina, F. H.; Romsted, L. S. Ion Binding and Reactivity at Charged Aqueous Interfaces. *Acc. Chem. Res.* **1991**, *24*, 357–364.
- (11) Romsted, L. S. *Introduction to Surfactant Self-Assembly*; Wiley and Sons: New York, 2012; Vol. 1.
- (12) Laguerre, M.; Bayrasy, C.; Lecomte, J.; Chabi, B.; Decker, E. A.; Wrutniak-Cabello, C.; Cabello, G.; Villeneuve, P. How to Boost Antioxidants by Lipophilization? *Biochimie* **2013**, *95*, 20–26.
- (13) Jonsson, B.; Lindman, B.; Holmberg, K.; Kronberg, B. *Surfactants and Polymers in Aqueous Solution*; John Wiley & Sons: Chichester, U.K., 1998; Table 2.8, p 55.
- (14) Romsted, L. S. Micellar Effects on Reaction Rates and Equilibria, In *Surfactants in Solution*; Mittal, K. L., Lindman, B., Eds.; Plenum Press: New York, 1984; Vol. 2, pp 1015–1068.
- (15) Savelli, G.; Germani, R.; Brinchi, L. Reactivity Control by Aqueous Amphiphilic Self-Assembling Systems, In *Reactions and Synthesis in Surfactant Systems*; Texter, J., Ed.; Marcel Dekker: New York, 2001; Vol. 100, pp 175–246.
- (16) Menger, F. M.; Portnoy, C. E. On the Chemistry of Reactions Proceeding Inside Molecular Aggregates. *J. Am. Chem. Soc.* **1967**, *89*, 4698–4703.
- (17) Martinek, K.; Yatsimirski, A. K.; Levashov, A. V.; Berezin, I. V. The Kinetic Theory and the Mechanisms of Micellar Effects on Chemical Reactions, In *Micellization, Solubilization, and Microemulsions*; Mittal, K. L., Ed.; Plenum Press: New York, 1977; Vol. 2, pp 489–508.
- (18) Romsted, L. S. Rate Enhancements in Micellar Systems. Ph.D. Thesis, Indiana University, 1975.
- (19) Romsted, L. S. A General Kinetic Theory of Rate Enhancements for Reactions between Organic Substrates and Hydrophilic Ions in Micellar Solutions, In *Micellization, Solubilization and Microemulsions*; Mittal, K. L., Ed.; Plenum Press: New York, 1977; Vol. 2, pp 489–530.
- (20) Quina, F. H.; Chaimovich, H. Ion Exchange in Micellar Solutions. 1. Conceptual Framework for Ion Exchange in Micellar Solutions. *J. Phys. Chem.* **1979**, *83*, 1844–1850.
- (21) Bunton, C. A. Micellar Rate Effects upon Organic Reactions, In *Kinetics and Catalysis in Microheterogeneous Systems: Surfactants in Science Series*; Gratzel, M., Kalyanasundaram, K., Eds.; Marcel Dekker: New York, 1991; Vol. 38, pp 13–47.
- (22) Bunton, C. A. The Dependence of Micellar Rate Effects upon Reaction Mechanism. *Adv. Colloid Interface Sci.* **2006**, *123–126*, 333–343.
- (23) da Rocha Pereira, R.; Zanette, D.; Nome, F. Application of the Pseudophase Ion-Exchange Model to Kinetics in Microemulsions of Anionic Detergents. *J. Phys. Chem.* **1990**, *94*, 356–361.
- (24) Romsted, L. S.; Zhang, J. Kinetic Method for Determining Antioxidant Distributions in Model Food Emulsions: Distribution Constants of t-Butylhydroquinone in Mixtures of Octane, Water and a Nonionic Emulsifier. *J. Agric. Food. Chem.* **2002**, *50*, 3328–3336.
- (25) Quina, F. H. Dynamics and Prototropic Reactivity of Electronically Excited States in Simple Surfactant Aggregates. *Curr. Opin. Colloid Interface Sci.* **2013**, *35*–39.
- (26) Anslyn, E. V.; Dougherty, D. A. *Modern Physical Organic Chemistry*; University Science Books: Sausalito, CA, 2006; Table 3.5, p 157.
- (27) Bender, M. L. *Mechanisms of Homogeneous Catalysis from Protons to Proteins*; Wiley-Interscience: New York, 1971.
- (28) Laidler, K. J. *Chemical Kinetics*; Harper & Row: New York, 1987; p 211.
- (29) Lorand, J. On the Absolute Reactivity of Aryl Cations: Selectivity Toward Halide Ions as a Function of Viscosity. *Tetrahedron Lett.* **1989**, *30*, 7337–7340.
- (30) Quina, F. H.; Lissi, E. A. Photoprocesses in Microaggregates. *Acc. Chem. Res.* **2004**, *37*, 703–710.
- (31) Frankel, E. N. *Lipid Oxidation*; The Oily Press: Dundee, 2005.
- (32) Losada-Barreiro, S.; Sanchez-Paz, V.; Bravo-Diaz, C. Effects of Emulsifier Hydrophile-Lipophile Balance and Emulsifier Concentration on the Distributions of Gallic acid, Propyl Gallate, and alpha-Tocopherol in Corn Oil Emulsions. *J. Colloid Interface Sci.* **2013**, *389*, 1–9.
- (33) Choe, E.; Min, D. B. Mechanisms of Antioxidants in the Oxidation of Foods. *Compr. Rev. Food Sci. Food Saf.* **2009**, *8*, 345–358.
- (34) Losada-Barreiro, S.; Bravo-Diaz, C.; Paiva Martins, F.; Romsted, L. S. A Maximum in Antioxidant Distributions and Efficiencies with Increasing Hydrophobicity of Gallic Acid and its Alkyl Esters. The Pseudophase Model Interpretation of the "Cut-Off" Effect. *J. Agric. Food. Chem.* **2013**, *61*, 6533–6543.
- (35) Pastoriza-Gallego, M. J.; Losada-Barreiro, S.; Bravi-Diaz, C. Effects of Acidity and Emulsifier Concentration on the Distribution of Vitamin C in a Model Food Emulsion. *J. Phys. Org. Chem.* **2012**, *25*, 908–915.
- (36) Losada-Barreiro, S.; Paz, V. S.; Bravi-Diaz, C.; Martins, F. P. Temperature and Emulsifier Concentration Effects on Gallic Acid Distribution in a Model Food Emulsion. *J. Colloid Interface Sci.* **2012**, *370*, 73–79.
- (37) Lisete-Torres, P.; Losada-Barreiro, S.; Albuquerque, H.; Sanchez-Paz, V.; Paiva-Martins, F.; Bravo-Diaz, C. Distribution of Hydroxytyrosol and Hydroxytyrosol Acetate in Olive Oil Emulsions and Their Antioxidant Efficiency. *J. Agric. Food. Chem.* **2012**, *60*, 7318–7325.
- (38) Gunaseelan, K.; Romsted, L. S.; Gallego, M. J. P.; Gonzalez-Romero, E.; Bravo-Diaz, C. Determining α -Tocopherol Distributions between the Oil, Water, and Interfacial Regions of Macroemulsions: Novel Applications of Electroanalytical Chemistry and the Pseudophase Kinetic Model. *Adv. Colloid Interface Sci.* **2006**, *123*, 303–311.
- (39) Zollinger, H. *Diazo Chemistry I: Aromatic and Heteroaromatic Compounds*; VCH Publishers: Weinheim, 1994.
- (40) Romsted, L. S. Interfacial Composition of Surfactant Assemblies by Chemical Trapping with Arenediazonium Ions: Method and Applications, In *Reactions and Synthesis in Surfactant Systems*; Texter, J., Ed.; Marcel Dekker: New York, 2001; pp 265–294.
- (41) Romsted, L. S. Do Amphiphile Aggregate Morphologies and Interfacial Compositions Depend Primarily on Interfacial Hydration and Ion Specific Interactions? The Evidence from Chemical Trapping. *Langmuir* **2007**, *23*, 414–424.
- (42) Zhang, Y.; Romsted, L. S.; Zhuang, L.; de Jong, S. Simultaneous Determination of Interfacial Molarities of Amide Bonds, Carboxylate Groups, and Water by Chemical Trapping in Micelles of Amphiphiles Containing Peptide Bond Models. *Langmuir* **2012**, *29*, 534–544.
- (43) Gunaseelan, K.; Romsted, L. S.; Gonzalez-Romero, E.; Bravo-Diaz, C. Determining Partition Constants of Polar Organic Molecules Between the Oil/Interfacial and Water/Interfacial Regions in Emulsions: A Combined Electrochemical and Spectrometric Method. *Langmuir* **2004**, *20*, 3047–3055.
- (44) Bravo-Diaz, C. Diazo Ethers: Formation and Decomposition in the Course of Reactions between Arenediazonium Ions and Different Alcohols. *Mini-Rev. Org. Chem.* **2009**, *6*, 105–113.
- (45) Costas-Costas, U.; González-Romero, E.; Bravo-Díaz, C. Sodium Dodecyl Sulfate Micellar Effects on the Reactivity of Arenediazonium Ions with Ascorbic Acid Derivatives. *Langmuir* **2003**, *19*, 5197–5203.
- (46) Costas-Costas, U.; Bravo-Díaz, C.; Gonzalez-Romero, E. Micellar Effects on the Reaction Between an Arenediazonium Salt and 6-Octanoyl-L-Ascorbic Acid. Kinetics and Mechanism of the Reaction. *Langmuir* **2004**, *20*, 1631–1638.
- (47) Costas-Costas, U.; Bravo-Díaz, C.; Gonzalez-Romero, E. Kinetics and Mechanism of the Reaction between Ascorbic Acid Derivatives and an Arenediazonium Salt: Cationic Micellar Effects. *Langmuir* **2005**, *21*, 10983–10991.

- (48) Pastoriza-Gallego, M. J.; Fernandez-Alonso, A.; Losada-Barreiro, S.; Sanchez-Paz, V.; Bravo-Diaz, C. Kinetics and Mechanism of the Reaction between 4-Hexadecylbenzenediazonium Ions and Vitamin C in Emulsions: Further Evidence of the Formation of Diazo Ether Intermediates in the Course of the Reaction. *J. Phys. Org. Chem.* **2008**, *21*, 524–530.
- (49) Brown, K. C.; Doyle, M. P. Reduction of Arenediazonium Salts by Hydroquinone. Kinetics and Mechanism for the Electron-Transfer Step. *J. Org. Chem.* **1988**, *53*, 3255–3261.
- (50) Pastoriza-Gallego, M. J.; Sanchez-Paz, V.; Romsted, L. S.; Bravo-Diaz, C. Distribution of tert-Butylhydroquinone in a Corn Oil/C₁₂E₆/Water Based Emulsion. Application of the Pseudophase Kinetic Model. *Prog. Colloid Polym. Sci.* **2011**, *138*, 33–38.
- (51) Sanchez-Paz, V.; Pastoriza-Gallego, M. J.; Losada-Barreiro, S.; Bravo-Diaz, C.; Gunaseelan, K.; Romsted, L. S. Quantitative Determination of α -Tocopherol distribution in a Tributyrin/Brij 30/Water Model Food Emulsion. *J. Colloid Interface Sci.* **2008**, *320*, 1–8.
- (52) Frankel, E. N.; Huang, S.-W.; Kanner, J.; German, J. B. Interfacial Phenomena in the Evaluation of Antioxidants: Bulk Oils vs Emulsions. *J. Agric. Food. Chem.* **1994**, *42*, 1054–1059.
- (53) Costa, M.; Losada-Barreiro, S.; Paiva-Martins, F.; Bravi-Diaz, C. Effects of Acidity, Temperature and Emulsifier Concentration on the Distribution of Caffeic Acid in Stripped Corn and Olive Oil-in-Water Emulsions. *J. Am. Oil Chem. Soc.* **2013**, *90*, 1629–1636.
- (54) *Handbook of Chemistry and Physics*, 80th ed.; Lide, D. R., Ed.; CRC Press: Boca Raton, 1999.
- (55) Fazary, A. E.; Ju, Y. Nonaqueous Solution Studies on the Protonated Equilibria of Some Phenolic Acids. *J. Solution Chem.* **2008**, *37*, 1305–1309.
- (56) Ozkorucuklu, S. P.; Beltran, J. L.; Fonrodona, G.; Barron, D.; Alsancak, G.; Barbosa, J. Determination of Dissociation Constants of Some Hydroxylated Benzoic and Cinnamic Acids in Water from Mobility and Spectroscopic Data Obtained by CE-DAD. *J. Chem. Eng. Data* **2009**, *54*, 807–811.
- (57) Jaiswal, P. V.; Srivastava, A. K. Effects of Surfactants on the Dissociation Constants of Ascorbic and Maleic Acids. *Colloids Surf, B* **2005**, *46*, 45–51.
- (58) Cabrera, J. W.; Sepulveda, L. Transfer Free Energies of p-Alkylphenols and p-Alkylphenoxides from Water in Mixed Micelles Formed by a Cationic and Nonionic Surfactant. *Langmuir* **1989**, *6*, 240–243.
- (59) Boichenko, A. P.; Dung, L. T. K.; Loginova, L. P. Solubilization of Aliphatic Carboxylic Acids (C₃-C₆) by Sodium Dodecyl Sulfate and Brij 35 Micellar Pseudophases. *J. Solution Chem.* **2011**, *40*, 968–979.
- (60) Dupont-Leclercq, L.; Giroux, S.; Rubini, P. Solubilization of Amphiphilic Carboxylic Acids in Nonionic Micelles: Determination of Partition Coefficients from pK_a Measurements and NMR Experiments. *Langmuir* **2007**, *23*, 10463–10470.
- (61) Gu, Q.; Bravo-Diaz, C.; Romsted, L. S. Using the Pseudophase Kinetic Model to Interpret Chemical Reactivity in Ionic Emulsions: Determining Antioxidant Partition Constants and Interfacial Rate Constants. *J. Colloid Interface Sci.* **2013**, *400*, 41–48.
- (62) Laidler, K. J.; Meiser, J. H.; Sanctuary, B. C. *Physical Chemistry*, 4th ed.; Brooks/Cole: Belmont, 2002.
- (63) Drinkel, E.; Souza, F. D.; Fiedler, H. D.; Nome, F. The Chameleon Effect in Zwitterionic Micelles: Binding of Anions and Cations and Use as Nanoparticle Stabilizing Agents. *Curr. Opin. Colloid Interface Sci.* **2013**, *18*, 26–34.
- (64) Gu, Q.; Romsted, L. S. Unpublished results, 2015.
- (65) McClements, D. J. *Food Emulsions: Principles, Practices, and Techniques*, 2nd ed.; CRC Press, 2004.
- (66) Martinez-Aranda, N.; Barreiro, S. L.; Bravo-Diaz, C.; Romsted, L. S. Influence of Temperature on the Distribution of Catechin in Corn Oil-in-Water Emulsions and Some Relevant Thermodynamic Parameters. *Food Biophys.* **2014**, *9*, 380–388.
- (67) Pastoriza-Gallego, M. J.; Sanchez-Paz, V.; Losada-Barreiro, S.; Bravo-Diaz, C.; Gunaseelan, K.; Romsted, L. S. Effects of Temperature and Emulsifier Concentration on α -Tocopherol Distribution in a Stirred, Fluid, Emulsion. Thermodynamics of α -Tocopherol Transfer between the Oil and Interfacial Regions. *Langmuir* **2009**, *25*, 2646–2653.
- (68) Leo, A.; Hansch, C.; Elkins, D. Partition Coefficients and Their Uses. *Chem. Rev.* **1971**, *71*, 525–616.
- (69) Costa, M.; Losada Barreiro, S.; Paiva-Martins, F.; Bravo-Diaz, C.; Romsted, L. S. A Direct Correlation between the Antioxidant Efficiencies of Caffeic Acid and Its Alkyl Esters and Their Concentrations in the Interfacial Region of Olive Oil Emulsions. The Pseudophase Model Interpretation of the “Cut-Off” Effect. *Food Chem.* **2015**, *175*, 233–242.